Supplementary Materials for

HEM1 deficiency disrupts mTORC2 and F-actin control in inherited immunodysregulatory disease

Sarah A. Cook[1*], William A. Comrie[1,25*], M. Cecilia Poli[2,3,4], Morgan Similuk[5], Andrew J. Oler[6], Aiman J. Faruqi[1], Douglas B. Kuhns[7], Sheng Yang[8], Alexander Vargas-Hernández[2,3], Alexandre F. Carisey[2,3], Benjamin Fournier[9,10], D. Eric Anderson[11], Susan Price[12], Margery Smelkinson[24], Wadih Abou Chahla[13], Lisa R. Forbes[2,3], Emily M. Mace[14], Tram N. Cao[2,3], Zeynep H. Coban-Akdemir[15,16], Shalini N. Jhangiani[16,17], Donna M. Muzny[16,17], Richard A. Gibbs[15-17], James R. Lupski[15-17], Jordan S. Orange[14], Geoffrey D.E. Cuvelier[18], Moza Al Hassani[19], Nawal AL Kaabi[19], Zain Al Yafei[19], Soma Jyonouchi[20], Nikita Raje[21], Jason W. Caldwell[22], Yanping Huang[23,26], Janis K. Burkhardt[23], Sylvain Latour[9,10], Baoyu Chen[8], Gehad ElGhazali[19], V. Koneti Rao[12], Ivan K. Chinn[2,3], Michael J. Lenardo[1]

correspondence to: lenardo@nih.gov

This PDF file includes:

Other Supplementary Materials for this manuscript includes the following:

Materials and Methods

Study participants and human sample collection

We enrolled five patients from four families from living in Canada, the United States, the United Arab Emirates, and France. Patients were included in the study based on a molecular identification of function-affecting variants in *NCKAP1L*. The ages of the patients ranged from 3 to 18 years as of May 2020. Patients were initially identified on the basis of recurrent infections, Epstein–Barr virus (EBV)-driven hemophagic lymphohistiocytosis (HLH), and/or lymphoproliferative disease resembling an ALPS-like phenotype. Whole exome DNA sequencing (WES) was carried out following initial clinical evaluation and in three cases, negative screening results for ALPS-causal mutations. For details regarding individual patients, see the individual patient narratives in the supplemental material available with the full text of this article. All human subjects (or their legal guardians) provided written informed consent in accordance with Helsinki principles for enrollment in research protocols that were approved by the Institutional Review Boards of the National Institute of Allergy and Infectious Diseases, National Institutes of Health (NIH), Baylor College of Medicine (BCM), and collaborating institutions. Patient or healthy control samples were obtained from the NIH Clinical Center or other institutions overseeing patient care under approved protocols and shipped to the NIH. Mutations will be archived by Online Mendelian Inheritance in Man (OMIM) at time of publication, and whole-exome data has been submitted in dbGaP.

Genomic analysis

Genomic DNA (gDNA) was obtained from probands and family members by isolation and purification from peripheral blood mononuclear cells (PBMCs) using Qiagen's DNeasy Blood and Tissue Kit or similar kit. DNA was then submitted for WES through either the NIH Clinical Center, BCM, or via a commercial service. WES was performed on all patients and was combined with homozygosity/ loss of heterozygosity mapping. All sequenced DNA reads were mapped to the human genome reference. Single-nucleotide variant (SNV) and indel were called and SNVs/indels were annotated, filtered, and prioritized for autosomal recessive putative disease-causing variants based on the pedigree analysis using a custom GEMINI pipeline (*30).*

The probability of intolerance to heterozygous Loss- of-f Function variation Intolerance (pLI) score for NCKAP1L was 0.85 in the Genome Aggregation Database (gnomAD), indicating it is intolerant of sequence changes and is essential for human health (*31*). Patient (Pt) 1.1 was homozygous for a missense variant

(NM_005337.4:c.1076C>T) resulting in a p.Pro359Leu (P359L) substitution. Pt 2.1 and Pt 2.2 are were compound heterozygous for P359L along with a second variant allele (NM_005337.4:c.1555G>C) causing a p.Val519Leu (V519L) substitution. Pt 3.1 was homozygous for a single nucleotide change (NM_005337.4:c.1111A>G) resulting in a p.Met371Val (M371V) substitution. Pt 4.1 was homozygous for a fourth variant (NM_005337.4:c.773G>T) resulting in a p.Arg258Leu (R258L) substitution.

Cells, Media, and Cell Culture

Stimulation Buffer (SB) (Hepes buffered saline, 1% BSA, 0.1% fetal bovine serum (FBS), 2 mM $MgCl_2$, 1 mM $CaCl_2$, 6 mM Glucose) was used for all in vitro short term stimulations. DMEM, RPMI, or X-Vivo15 media were supplemented with 10% FBS, 1% L-glutamine (2 mM), 1% pen–strep (all Invitrogen) and 50 μM 2-ME (Sigma) to make complete media. Complete RPMI was supplemented with 100 I.U./ml IL-2 (Roche) for primary cell culture or 20% FBS for growth of B lymphoblastoid cell lines (BLCL). HEK293T cells and Jurkat E6.1 cells (ATCC) and were cultured in complete DMEM and complete RPMI, respectively. NKL cells were grown in complete RPMI supplemented with 100 I.U./ml IL-2. LentiX-293T were purchased from Clontech and were cultured in complete DMEM. The mouse mastocytoma P815 target cell line was from ATCC and cultured in complete DMEM. EBV-transformed B cell lines were generated from patient PBMC by transformation with B95-8 EBV cell supernatant and cultured in RPMI medium with 20% FBS, 2 mM glutamine, and 1 μg/ml cyclosporin A. K562 cell lines used as target cells for Cr^{51} release assays and NK cell conjugate analysis by confocal microscopy were maintained in RPMI media supplemented with 10% FCS. PBMCs were isolated from anti-coagulated blood by Ficoll® Paque density separation by centrifugation at 800 × *g* for 20 min followed by collection of the buffy coat layer and three washes of 50 ml phosphate-buffered saline (PBS). PBMCs were then immediately used or frozen at 2-5 × 10^7/ml in freezing media (90% FBS and 10% DMSO). Human T cells were isolated from fresh or frozen PBMCs using the appropriate kit from Miltenyi Biosciences according to the manufacturer's protocol (Naïve $CD4^+$, Naïve $CD8^+$, PanT, and Pan $CD4^+$). Purity of cells was verified by flow cytometry. Human T cells were then either used immediately for functional studies or activated by CD3/28 magnetic beads, 1 bead per 2 cells, (Invitrogen) and expanded in complete RPMI supplemented with IL-2. T cell blasts were used for functional analysis between 1 and 3 weeks post activation. Patient and control neutrophils were isolated by density

gradient separation and used immediately for experiments. In all cases when patient T cells were compared to control T cells, naïve T cells ($CD4^+$ or $CD8^+$) were isolated and used either immediately or expanded to T cell blasts in order to prevent issues arising from altered cell subsets in patients versus healthy donors.

HEM1 or WAVE2 deficient Jurkat E6.1 Cells and HEM1-deficient NKL lines were generated by CRISPR RNP-mediated deletion followed by single cell cloning. Guide RNAs against HEM1 and WAVE2 were generated by using IDT's online tool and the top two sequences were pooled following resuspension for a 100 μM final stock solution. Guide RNA was mixed 1:1 with fluorescent tracrRNA (IDT) and heated to 95°C for 5 min then allowed to cool to room temperature. Nine microliters of the tracr/guide complexes were added to 3 μl of purified Cas9 protein (30 μg) and 3 μl of duplex buffer (both IDT). Jurkat T cells or NKL cells (1×10^7) were electroporated using the P2 primary Cell 4D-nucleofector kit from Lonza with program EH-100. Cells were allowed to recover, and then cloned by serial dilution and screened for loss of HEM1 or WAVE2 by flow cytometry and immunoblotting. Cell lines were confirmed as mycoplasma-negative before their use in experiments using a PCR-based assay (Sigma Aldrich).

Plasmids and Cloning

The pLV-EF1a-IRES-puro, GFP-Flag expression vector, Myc-RICTOR expression vector, pcDNA3.1-ccdB-3xFLAG-V5, and the two RICTOR shRNA vectors were purchased from Addgene. The pEnter/D-TOPO entry vector was purchased from Thermo Fischer. shRNA vectors against HEM1, the lentiviral packaging constructs (pMD2.G and psPAX2), and the Lifeact-GFP expression construct were a kind gift from J.K. Burkhardt.

Full-length HEM1 was PCR-amplified from cDNA prepped from T cells from a healthy control using Qiagen's RNeasy kit and the SuperScript-III First Strand Synthesis System for RT-PCR (Invitrogen) using random hexamers and the manufacturer's protocols. To amplify full length HEM1, touchdown PCR amplification with Phusion Flash polymerase (Thermo Fisher) was performed using with the following primers, F-5′-CACCATGTCTTTGACATCTGCTTAC-3′, and reverse, 5′-CAGTTTAGGTGGAAGGCCCGAG-3′. The PCR product was gel purified and directionally cloned into the

pENTR/D-TOPO Gateway cloning vector using the the pENTR/D-TOPO Cloning Kit with One-Shot/TOP10 chemically competent cells (Thermo Fisher). The WT-sequence was verified by Sanger sequencing. The P359L, M371V, V519L mutants were produced by site-directed mutagenesis of the WT sequence using the following primers:

P359L:

F-5′-GATGAACTGGGACTACTGGGTCCTAAGGCT-3′

R-5′-GTAGTCCCAGTTCATCAGCCAACACAGTCTC-3′

M371V:

F-5′-TGCTTTCGTGGCCCTGTCCTTCATTCGTG-3′

R-5′-CAGGGCCACGAAAGCAAAAAGAGCCTTAGG-3′

V519L:

F-5′-GGAGTGGAAGAGAATGAGGTTCATCACCTTGGC-3′

R-5′- GCCAAGGTGATGAACCTCATTCTCTTCCACTCC-3′

HEM1 expression constructs containing C-terminal 3xFLAG-v5 tags were generated in a pcDNA3.1 backbone (Addgene) using Gateway cloning technology (Thermo Fisher) as follows. First, WT HEM1 was PCR amplified using the WT forward primer listed above and a reverse primer that removed the stop codon: (R-5′-GTTTAGGTGGAAGGCCCGAGACACCT-3′). This product was gel purified using the NucleoSpin Gel and PCR Cleanup Kit (Machinery-Nagel) and cloned into the pENTR/D-TOPO Gateway cloning vector via the BP-Clonase reaction. Finally, HEM1 sequences were shuttled to the pcDNA3.1 destination vector containing a C-terminal 3xFLAG-v5 tag via the LR-Clonase reaction.

Lentiviral constructs were generated in a pLV-EF1a-IRES-puro backbone using InFusion cloning technology (Takara Bio). Briefly, C-terminally FLAG-tagged HEM1 sequences were amplified using the following primers: (F-5′-TAGATCGCGAACGCGATGTCTTTGACATCTGCTTACCAGC-3′; R-5′-CGCCCTCGAGGAATTTGTAGAATCGAGACCGAGGAGAGG-3′). After gel purification, HEM1 PCR products were incubated with the InFusion Enzyme and linearized pLV-EF1a-IRES-puro backbone previously digested with EcoRI and MluI. All constructs were verified by Sanger sequencing.

Plasmid Transfection and Lentiviral Production/Transduction

For HEM1 overexpression experiments, 2×10^6 HEK293T cells were transiently transfected with 20 μg HEM1-3x FLAG plasmid DNA using Lipofectamine 3000 reagent (Thermo Fisher) and cultured for 72 hours before harvest. For Rictor overexpression experiments, 2×10^6 HEK293T cells stably expressing FLAG-tagged HEM1 were transiently transfected with 2 μg myc-RICTOR plasmid (Addgene). Control HEK293T cells were transfected with myc-Rictor or 10 ng GFP-3xFLAG as described. Lifeact-GFP was transiently transfected into primary T cell blasts using the Amaxa 96-well shuttle system (Lonza) and the recommended protocol for activated human T cells.

For production of lentiviruses, LentiX-293T cells (Takara Bio) were grown to 80% confluency and transfected with 4 μg pMD2.G, 14 μg psPAX2, and 18 μg of lentiviral expression or knockdown vectors using Lipofectamine 3000 reagent (Invitrogen), according to the manufacturer's protocol. Culture supernatants containing lentiviruses were harvested after 72 hours, clarified by centrifugation for 15 min at $700 \times g$ and stored at −80°C until use.

For generation of stable HEM1-mutant expressing Jurkat cells, HEM1-knockout Jurkat cells were seeded in 24-well plates in RPMI supplemented with 8 μg/ml Polybrene (Sigma) and 1 ml of HEM1-containing lentiviruses. Plates were centrifuged for 2 hours at $800 \times g$ at 32°C. Transduced cells were cultured in complete RPMI for 48 hours before being maintained in 1 μg/ml puromycin selection for at least 48 hours. The same procedure was used to transduce Jurkat cell lines with LifeAct-GFP, HEK293T cells with HEM1-3XFLAG constructs, and primary T cells with shRNA constructs.

Inhibitors and Inhibitor Treatments

Inhibitors were added to T cells 30 min prior to restimulation and kept in culture during the duration of the T cell stimulation. A vehicle-only control was included equivalent to the highest volume used in the inhibitor-treated cells. The PI3Kβ/δ inhibitor AZD 8186 was purchased from Selleckchem and used at a final concentration of 100 μM, The AKT inhibitor MK-2206 H-Cl was purchased from Selleckchem and used at a final concentration of 10 μM. Rapamycin was purchased from Selleckchem and used at a final concentration of 1 μM. The mTOR-catalytic inhibitor KU-0063794 was purchased from Selleckchem and

used at a final concentration of 10 μM. Latrunculin A was purchased form Sigma and used at the indicated concentrations. Lck inhibitor was purchased from Millipore and used at a final concentration of 10 μM. The pan-Jak inhibitor (CAS 457081-03-7) was purchased from Sigma/Millipore and was used at a final concentration of 1mM. All inhibitors were resuspended in dimethyl sulfoxide (DMSO) and single use stock solutions were kept at −20°C.

$CD8^+$ T cell Cytotoxicity

$CD8^+$ T cell blasts, originally derived from purified naïve $CD8^+$ T cells, from normal controls and patients were collected, rested for 3 hours in basal RPMI, and resuspended to 1×10^6/ml and serial dilutions were prepared for addition of target cells. P815 cells (ATCC) were collected by gentle lifting in PBS with ethediamine tetraacetic acid (EDTA) and a single cell suspension was generated by repeat pipetting and passage through a 70 μM filter. Cells were then either left alone or coated with 1 μg/ml anti-CD3 for 30 min on ice in basal RPMI. Cells were washed three times with complete media and resuspended to 1×10^6/ml in complete RPMI. Target cells (5×10^4) were then added to a 96-well V-bottom plate in triplicate for each dose or donor. T cells were then added to reach the appropriate effector to target ratio. The volume was held constant at 200 μL. Controls included target cells with no anti-CD3 coating, absence of cells, effector only spontaneous lysis, a target cell spontaneous lysis only control, and a maximal target cell lysis control. Cells were allowed to incubate at 37°C for 4 to 6 hours. Cytotoxicity was then measured by release of lactate dehydrogenase into the supernatant from dying cells based on the CytoTox 96® Non-Radioactive Cytotoxicity assay from Promega. Percent cytotoxicity was calculated as described in the product insert and normalized to the results obtained from the control cells and averaged across multiple experiments.

^{51}Cr release assays to analyze NK cell-mediated cytotoxicity

Chromium release assays were used to determine NK cell cytotoxicity as previously described (*32).*

Frozen PBMCs were thawed, left to rest for 3 hours at 37°C and 5% CO_2. Resting cells were counted and incubated at varying ratios (50:1, 25:1, 12.5:1, 6.25:1, and 3.13:1) with 10^4 K562 target cells that were previously labeled with 50 mCi of ^{51}Cr and then washed. Where indicated, assays were performed in the presence of 1000 I.U./ml IL-2 (Roche). Effector-target conjugates were incubated in 200 ml in round-bottom

96-well plates (Corning, Corning). After 4 hours of incubation, positive controls for maximal lysis were produced by lysing labeled target cells with 1% octylphenoxypolyethoxyethanol. Supernatants were harvested and transferred to LumaPlates (PerkinElmer). The supernatant was dried, and plates were read on a TopCount gamma counter (PerkinElmer). Values were plotted using GraphPad Prism 7 software. Values were normalized to the percentage of NK cells in the initial PBMC population to calculate the lytic units.

NK synapse analysis

See Table S6 for a complete list of antibodies used in this study. Conjugate staining was performed as previously described (*33, 34*). Briefly, PBMCs from patients were incubated with susceptible K562 target cells for 15 min in a conical tube at 37°C and 5% CO_2 and subsequently mounted on a slide for 20 min at 37°C and 5% CO_2 to facilitate conjugate formation. After incubation, cells were fixed, permeabilized, and stained intracellularly with anti-WAVE2 rabbit primary antibody (Cat #3659, CST) followed by AlexaFluor-568 goat anti-rabbit secondary antibody diluted 1:1000 (Cat #A11011, Invitrogen), anti-perforin–AlexaFluor-488 diluted 1:50 (Cat #308108, BioLegend), and phalloidin–AlexaFluor-647 diluted 1:100 (Cat #A22287, Invitrogen). Slides were mounted using ProLong Glass antifade reagent (ThermoFisher Scientific) and #1.5 glass cover slips (Corning) and cured for 24 hours prior to observation by confocal microscopy. Fixed cells were imaged using a Zeiss Axio Observer Z.1 microscope stand equipped with a Yokogawa CSU10 spinning disk and a Hamamatsu Orca-R2 C10600 CCD camera. Laser lines used include 405, 488, 561 and 647 nm Coherent OBIS LX powered by a MultiLine LaserBank (Cairn Research). Emitted light was selected using the following filters as appropriate for the relevant dye: 460/50, 520/35 and 593/40 (Chroma Technology Corp). Imaging was performed using the plan apochromatic 63× 1.4NA oil immersion objective and MetaMorph software (v. 7.8.13; Molecular Devices) was used for hardware control and image acquisition. Images were taken in multiple *z*-planes and stacked for analysis. Raw 3D stacks of images were exported for processing and analysis in Fiji (*35*) using a custom script. Briefly, binary masks of individual cells were created using the threshold tool applied to the F-actin detection fluorescent channel. Cell outlines were filtered using a size cut-off (>10 μm^2). The fluorescence intensity of the Actin and WAVE2 staining channels for each cell was then measured for the sum of all planes of the 3D stack within the

Immune synapse mask outline, and plotted using GraphPad Prism. For display purposes only, raw 3D stacks were reduced to a single plane using a maximum projection transformation and subjected to a linear scaling of their intensity, identically across all conditions, for optimal visualization.

Conjugation assay

K562 cells were labeled with 0.125 μM of Carboxyfluorescein succinimidyl ester (CFSE) (Molecular Probes) for 15 min at room temperature. PBMCs were pre-stained with anti-CD3-BV711 (40 μg/ml, 1 μl per test, clone OKT3, Cat #317328, Biolegend) and anti-CD56-BV605 antibody (100 μg/ml, 2 μl per test, clone HCD56, Cat #318334, Biolegend). PBMCs (10^6 cells) and 10^5 target cells were incubated at 37°C for 0, 10, 30, or 60 min in 200 μl of R10 medium, mixed very gently, and fixed with 1% paraformaldehyde (EMS). Finally, all samples were acquired with the LSR-Fortessa flow cytometer and analyzed using FlowJo.

NKL cell line studies

For cytokine secretion assays, NKL cells were collected, washed and rested for 3 hours in basal RPMI. Cells were then counted and resuspended to 10^6 cells/ml in complete X-vivo15 media. Cells were then either left unstimulated or stimulated with maxisorb-plate bound anti-NKG2D and anti-2B4 (1 μg/ml each) for 18-24 hours. At the indicated times, supernatants were collected and the indicated cytokine was measured by the CD8/NK cell Legendplex kit (Biolegend). Cytokine secretion was normalized to the control cell line responses. Granzyme A was constitutively secreted in the absence of stimulation but no other cytokine was detected at appreciable levels in the absence of exogenous stimulation. To stain for intracellular granzyme A, NKL cells were collected, rested for 3 hours and normalized to 10^6 cells/ml. Cells were treated with monensin (Biolegend) for 4 hours to prevent cytokine trafficking and release. After that time, cells are fixed in PFA, permeabilized with 0.2% Triton-X100, washed, and blocked with flow cytometry buffer. Staining antibody was added at 1:100 dilution for 2 hours at room temperature or overnight at 4°C. Cells were collected and analyzed by flow cytometry.

Preparation of Stimulatory Surfaces for Microscopy and T cell activation assays

For microscopy, glass slides or 8-well chambers were coated with either ICAM-1 alone or anti-CD3 (clone Hit3a from Biolegend)/anti-CD28 (clone CD28.2 from Biolegend)/ICAM-1 (R&D systems) in PBS for 2 hours at 37°C to analyze T cell migration or synapse formation, respectively. Slides were washed three times with PBS prior to use. To analyze T cell stimulation, proliferation, and cytokine secretion, 96-well MaxiSorp plates were coated with anti-CD28 with/without ICAM-1 (1 μg/ml each) and varying doses of anti-CD3 for 2 hours at 37°C, followed by three washes with PBS to remove unbound antibody.

T Cell Imaging

To image the T cell F-actin network during immune synapse formation in real time, patient or control T cell blasts, originally expanded from purified Naïve $CD4^+$ T cells, were transfected with Lifeact-GFP and 48 hours later were washed and resuspended in Stimulation Buffer and allowed to spread on anti-CD3/28/ICAM-1 coated surfaces, and T cell synapses were imaged using a 1 micron-thick *z*-stack around the area of cell-glass contact using a Leica SP8 at the NIAID microscopy core facility. To image T cells migrating randomly on immobilized ICAM-1 cells were resuspended in L-15 media (Lonza) supplemented with 6 mM Glucose and allowed to adhere to ICAM-1 coated chambers. Cells were then imaged with differential interference contrast microscopy and either a 63X objective with a 500-ms frame rate to visualize the dynamics of the leading edge of migrating cells or a 5X objective at a frame rate of 30 s to measure cell migratory behavior over a longer period of time and distance. Images were collected on a Zeiss Axiovert 200 M inverted microscope equipped with an MS-2000 automatic stage (Applied Scientific Instruments) and a 37°C environmental chamber using Slidebook (Intelligent Imaging Innovation). Images were acquired using a Coolsnap FX-HQ camera (Roper Scientific).For fixed cell imaging of the actin network, patient or control T cell blasts were allowed to spread on ICAM-1 (1 μg/ml) or anti-CD3/28/ICAM1 (1 μg/ml each) coated (1 μg/ml each) surfaces. Cells were allowed to spread or adhere for 10 min prior to washing away of loosely bound cells in prewarmed stimulation buffer and fixation in 3% paraformaldehyde (PFA)-PBS. Fixation was quenched with 50 mM NH_4Cl and cells were then permeabilized with 0.2% Triton X-100 in PBS. Following extensive washing and blocking in 2% bovine serum albumin (BSA)/1 mM EDTA in PBS, cells were stained with Phalloidin-AF647 or 594 for 30 min at room temperature, with or without addition of

anti-perforin-Alexa Fluor 488, washed and mounted with Fluoromount-G (Southern Biotech) prior to imaging as before.

Granule height quantification

T cells were stimulated, fixed, and stained with anti-perforin and phalloidin as described. Images were acquired using a Leica SP8 confocal equipped with a 63X/1.4NA objective, HyD detectors, as well as 488 nm, 594 nm, and 405 nm lasers. Images had a lateral and axial resolution of 103 nm and of 300 nm, respectively. Measuring the distance of perforin granules from the bottom of the cell was conducted using Imaris software (Bitplane). In brief, using the "Cell" feature, individual cells were first demarcated using the phalloidin, and when available, DAPI stains. Subsequently, Perforin was demarcated as vesicles within the cell. Distances of Perforin granules from the bottom of the cell could be calculated using the metrics "Z position relative to cell" which measures the distance of vesicles from the center of the cell and "Bounding Box AA" which measures the maximum height of the cell. Data was compiled and statistics were calculated using Microsoft Excel.

Ex vivo T cell Activation Assays

To analyze T cell CD25/CD69 upregulation as well as T cell proliferation, Naïve $CD4^+$ T cells (for Pt comparisons) or pan-CD4 T cells (for knockdown experiments) were first isolated from PBMCs and then labelled with CellTrace Violet (5 μM for 20 min). Cells were then resuspended to 10^6 cells/ml in complete RPMI and added to prepared maxisorp plates, 2-5 $\times$ 10^4 cells/well, technical replicates were included if enough cells were present). For CD25 and CD69 expression, cells were collected at 36 hours post activation, stained on ice with anti-CD25 (PE) and anti-CD69 (FITC) (Biolegend) for 45-60 min, washed repeatedly and analyzed by flow cytometry. For proliferation, cells were collected on day 5 or day 6 post activation, washed and resuspended in flow cytometry buffer (PBS / 2% FBS/ 1 mM EDTA). Immediately prior to collection, cells were stained with propidium iodide (PI) to mark dead cells. Populations were gated first on live cells by PI exclusion, then by forward scatter (FSC) and side scatter (SSC) followed by exclusion of doublets by FSC-A by FSC-H. For cytokine secretion, T cell blasts were activated for 7-21 days, rested for 3 hours in basal RPMI, and resuspended in X-vivo15 without IL-2. For T cell receptor (TCR) stimulation,

cells were added to prepared maxisorp plates with the indicated immobilized stimuli (1-5 $\times$ 10^5 cells/well). Supernatants were collected following an 18-24 hour stimulation. For stimulation by CD3/28 beads, PMA/I, or IL-2, cells were added to an uncoated 96-well tissue culture plate and the appropriate soluble stimuli were added for 18-24 hours prior to supernatant collection. For CD3/28 bead stimulation, stimulatory beads (Invitrogen) were added to cells at a ratio of 1:2, and mixtures were briefly centrifuged to encourage bead/cell interactions. PMA and Ionomycin were added to a final concentration of 10 ng and 1 μg/ml, respectively. For IL-2 stimulation, cells were plated and then 2X IL-2 containing X-vivo15 media was added for the indicated final concentration. Supernatants were analyzed by using either the Legendplex Multi-Analyte Flow Assay Kit for human CD8/natural killer (NK) cells or the human Th cytokine panel (Biolegend).

ICAM-1 Adhesion Assays

To analyze inside-out integrin activation, T cell blasts were washed three times in PBS (with Ca^{2+}/Mg^{2+}) and resuspended in stimulation buffer in the presence of 1 μg/ml AlexaFluor 647 conjugated F(ab′)2 goat anti-human Fc antibody (Jackson ImmunoResearch) with or without 2 μg/ml ICAM-1. Cells were left alone or stimulated with PMA (10 ng/ml) and ionomycin (1 μg/ml) and fixed after 10 min with a final concentration of 3% PFA. As a positive control for ICAM-1 binding, T cells were stripped of calcium and magnesium with 10 mM EDTA buffer and resuspended in stimulation buffer (SB) containing 1 mM Mn^{2+} supplementation in the place of Ca^{2+} and Mg^{2+}. Cells were incubated with ICAM-1 and the AlexaFluor 647 conjugated F(ab′)2 goat anti-human Fc antibody and fixed as before. ICAM-1 binding was measured by flow cytometry.

To analyze outside-in integrin activation, ICAM-1 was immobilized on maxisorp plates by first coating the plates overnight with 2 μg/ml anti-human Fc antibody (Jackson ImmunoResearch), washing three times with PBS, and then incubating with the indicated dose of ICAM-1 at 37°C for 2 hours. The plate was washed with SB and blocked in SB for 2 hours. While the plate was being prepared, primary $CD4^+$ or $CD8^+$ T cells were collected and rested in basal RPMI for 2-3 hours. Following the rest, cells were stained with 1 μM carboxyfluorescein succinimidyl ester (CFSE) for 10 min at room temperature. CFSE was then quenched with FBS, and the cells were extensively washed in SB to remove excess CFSE. Cells were placed on the ICAM-1-coated plate in triplicate, centrifuged for 2 min, and incubated at 37°C for 30 min. The plate was

washed gently with prewarmed SB 2-4 times, and fluorescence was measured by on a plate reader. ICAM-1 adhesion was expressed as a percentage of the maximum adhesion of control cells.

Analysis of NKL and T cell degranulation

NKL cells or cycling T cell blasts were rested for 3 hours in basal RPMI and then transitioned to stimulation media containing 1:100 dilution of anti-CD107a/Lamp-1 antibody or isotype control. Cells were then stimulated for 1 hour with PMA/I at 37°C. After 1 hour, PFA was added to a final concentration of 3% for 10 min. Cells were then washed three times with flow cytometry buffer to remove excess antibody and analyzed by flow cytometry.

Analysis of T cell signaling events

Relevant T cell blasts were removed from stimulatory beads at least 48 hours prior to reactivation and resuspended in fresh IL-2 containing media. Prior to the stimulation, dead cells were removed with the live/dead removal kit (Miltenyi) and cells were washed extensively with basal RPMI and rested at 37°C in basal media for at 3 hours in basal media. Cells were then resuspended in either basal media or stimulation buffer. For analysis of early signaling events by western blot, resuspended cells were stimulated with anti-CD3/28 (1 μg/ml each) and crosslinked with Protein A (0.2 μg/ml) for the indicated times. After the indicated time, cells were lysed in Triton X-100 lysis buffer and kept on ice until the end of the time course. Lysates were then cleared by centrifugation (21000 × *g* for 10 min), added to 4X reducing sample buffer, and heated for 5 min at 95°C. Samples were then analyzed by immunoblotting. For flow cytometry, cells were stimulated with the indicated crosslinked stimuli for the indicated time. Samples were then immediately fixed for 20 min with 3% PFA (final concentration), followed by quenching of the fixative, permeabilization for 30 min with ice-cold methanol, and blocking with flow cytometry buffer. Cells were then stained for 1-18 hours for the indicated phosphorylated proteins, washed three times with FACS buffer, and analyzed by flow cytometry. To analyze T cell calcium fluxes, T cell blasts from patients or normal controls were collected, washed and rested in basal RPMI, and then loaded with 0.5 μM indo-1 ratiometric calcium sensor (Thermo Fisher) in Powerload buffer (Thermo Fisher) for 20 min at room temperature followed by extensive washing to remove excess Indo-1. Cells were resuspended in SB lacking extracellular calcium or FBS. Cells were

then analyzed for calcium responses following TCR stimulation (10-s collection, addition of anti-CD3/28 antibodies, 20-s collection, addition of protein A crosslinker, 90-s collection, addition of 1 μM extracellular calcium, collected for total of 5 min) or following thapsigargin-induced release of Ca^{2+} stores (30-s of collection, addition of 1 μM thapsigargin, 90-s collection, addition of 1 μM extracellular calcium, collected for total of 5 min). Calcium levels were expressed as the ratio of fluorescent spectrum of the Indo-1 dye in the bound (396 nm) to unbound state (737 nm).

Analysis of IL-2 induced proliferation, CD25 and CD132 expression, and pSTAT3/5 activation

To analyze T cell proliferation downstream of the IL-2 receptor, patient or normal control $CD4^+$ T cell blasts were rested for 36 hours in complete RPMI in the absence of IL-2. Cells were then washed, labelled with 1 μM CFSE for 5 min at room temperature followed by quenching for 20 min with FBS and extensive washing, and removal of dead cells with the dead cell removal kit (Miltenyi). Cells were resuspended in complete RPMI with no IL-2 and plated at 2-5 $\times$ 10^4 cells/ well in a 96-well plate. IL-2-containing media was then added to the indicated final concentrations and cells were incubated at 37°C for 5 days, after which CFSE dilution was measured by flow cytometry. To analyze CD25/CD132 expression, cells were prepared as above without CFSE labeling. IL-2 (100 I.U./ml) was added to rested cells, and at the indicated times, cells were taken and fixed in PFA for 20 min. Following the completion of the time course cell pellets were resuspended in FACS buffer and stained with anti-CD25 (AlexaFluor 488) and anti-CD132 (PE) for 30 min, washed three times in flow cytometry buffer, and analyzed by flow cytometry. To measure pSTAT3/5 phosphorylation, patient and control T cell blasts previously transduced by lentivirus were collected, washed three times in basal RPMI, and rested for 3 hours in basal RPMI. Cells were then resuspended in basal RPMI at 1 $\times$ 10^6/m, plated in a 96-well V-bottom plate, and warmed to 37°C. IL-2 was added to cells at the indicated concentrations before fixing in PFA for 20 min, permeabilization in ice-cold methanol for 30 min, and extensive washing in flow cytometry buffer. Cells were then stained for pSTAT3 and pSTAT5 for 1 hour at RT and analyzed by flow cytometry.

Neutrophil chemotaxis

Neutrophil chemotaxis was measured using EZ-TAXIScan instrumentation (Effector Cell Institute, Tokyo, Japan) which monitors the migration of neutrophils across a 260 μm platform separating the "Cell" well from the "Chemoattractant" well. Isolated neutrophils (5×10^3 cells in 1.0 μL) were added to the "Cell" well of the EZ-TAXIScan and 1.0 μL of either buffer, fMLF (5×10^{-8} M), or C5a (5×10^{-8} M) was added to the opposing "Chemoattractant" well. Digital images of the migrating PMNs were captured every 30 s for 1 hour. Images were converted to stacks using the ImageJ software (version 1.46r; NIH). Ten randomly selected cells were electronically traced using the ImageJ plug-in, MTrackJ, and the sequential positional coordinates of individual migrating cells were determined as a function of time. The tracks of individual migrating cells were reconstructed and plotted with the position of each cell anchored at the origin at $t = 0$. Since data were collected with time and position, multiple parameters could be derived: overall distance, directed distance (parallel to the chemoattractant, random distance (orthogonal to the chemoattractant), overall velocity, directed and random velocity vectors, and time-to-event analysis (number of cells completing migration and elapsed time).

A modified Boyden chamber chemotaxis chamber was used to assess additional chemoattractants and doses. Purified neutrophils (10^7 cells/ml in Hank's balanced salt solution without divalent cations (HBSS)) were incubated with the cell-permeant fluorescent probe, calcein-AM (5 μM final) for 15 min in a 37ºC incubator wrapped in foil to protect from light. At the end of the incubation, the cells were washed, counted, and resuspended at 3×10^6/ml in 2% BSA/HBSS with divalent cations. The chemoattractants were diluted in 0.1% HSA in PBS and 29 μl of each chemoattractant was added to the bottom well of a 96-well ChemoTx® Disposable Chemotaxis System chamber that is fitted with a framed polycarbonate filter 6-10 μm in depth with 5.0 μm pores at a density of 4×10^5 pores/cm^2 (Neuro Probe, Inc., Gaithersburg, MD). The filter frame was replaced on the 96-well plate and 25 μl (75,000 cells) were pipetted onto an 8 mm^2 filter spot surrounded by a hydrophobic mask, forming a hemispherical droplet directly above the chemoattractant well. The chamber was incubated for 45 min at 37ºC, then the remaining cells were aspirated from atop the filter. EDTA (15 μl of 2 mM solution) was added to each filter spot and incubated additional 30 min at 4ºC to promote cell detachment from the filter. The EDTA was aspirated from the filter

and the chamber centrifuged for 5 min at 300 × *g*. The fluorescence of each well was determined using a fluorescent plate reader (Gemini EM, Molecular Devices, San Jose, Ca) using a $\lambda_{excitation}$ = 490 nm and $\lambda_{emission}$ = 520 nm. Fluorescence was converted to number of migrating cells using a standard curve of calcein-AM loaded cells. Neutrophil chemotaxis was analyzed with two different control donors in two independent experiments, the first of which was performed under Clinical Laboratory Improvement Amendments (CLIA) conditions for use as a clinical test,

Immunoblotting

To prepare lysates, cell pellets were either immediately lysed in 1% Triton X-100 buffer, 0.5% NP-40 buffer, or flash freeze-thawed five times before 25-min incubation in CHAPS lysis buffer (used for co-IP samples to maintain low affinity interactions). NKL, Jurkat E6.1, and primary T cells were lysed in 1% Triton X-100 (150 mM NaCl, 1% Triton X-100, 50 mM Tris pH 8.0 with protease and phosphatase inhibitor tablets (Roche)) when analyzing T cell signaling or 0.3% CHAPS buffer (0.3% CHAPS w/v, 40 mM HEPES pH 7.5, 120 mM NaCl, 1 mM EDTA with protease inhibitor tablet) for co-immunoprecipitation experiments. To analyze WRC interactions in overexpression experiments, HEK 293T cells were lysed in 0.5% NP40 lysis buffer (0.5% NP40 w/v, 150 mM NaCl, 50 mM Tris-Cl with protease inhibitor tablet). Following cell lysis for 15-25 min on ice, lysates were cleared by 10-15 min of centrifugation at 21000 × *g* at 4°C. Protein concentration of clarified lysates was determined using the Micro BCA Protein Assay Kit (Thermo Fisher). Samples were denatured in reducing (10% beta mercaptoethanol) NuPAGE LDS sample buffer (Thermo Fisher), boiled for 5 min at 95°C, and separated on 4-12% Bis-Tris gels (Invitrogen). Proteins were transferred to nitrocellulose membranes and blocked with 5% milk. Incubation with primary antibodies occurred for 2 hours at room temperature or overnight at 4°C, followed by a 1-hour incubation with goat anti-mouse AlexaFluor 680 or goat anti-rabbit AlexaFluor 800 secondary antibodies (Thermo Fisher). Alternatively, horseradish peroxidase anti-mouse or anti-rabbit secondary (Southern Biotech) were used to visualize proteins by chemiluminescence. Membranes were imaged on the Azure c500 Imaging System (Azure Biosystems) or exposed to autoradiography film and ImageJ software was used for all image analyses.

Immunoprecipitation

Lysates were prepared as described above. Clarified lysates (800-1000 μg) were incubated with primary antibody at 4°C for 1 hour, then for an additional 2 hours with magnetic Dynabeads Protein A (Thermo Fisher). Protein complexes were isolated, washed 3-5 times in lysis buffer, and immunoblotted as described or used in Mass-Spec analysis as described below.

Recombinant protein purification and biochemical assays

Recombinant human WRC containing full-length (FL) CYFIP1, FL HEM2, FL HSPC300, Abi2 (1-158) and WAVE1 (1-230)-$(GGS)_6$-(485-559), which we named WRC230VCA, was purified as previously described (*36*). The WRC containing M373V HEM2 behaved identically to the WT during expression and various chromatographic steps in purification, suggesting M373V did not affect folding, stability or WRC assembly. Other proteins, including the Arp2/3 complex, actin, WAVE1 VCA, GST-Tev-Rac1 (Q61L/P29S, 1-188), and Rac1 (Q61L/P29S, 1-188) were purified as previously described.(*36*) GST-thrombin-Arf1 (18-181) construct was obtained from Neal Alto's lab and was expressed and purified by following a similar protocol used for GST-Tev-Rac1 (*37*). Untagged Arf1 (18-181) was obtained from MBP-3C-Arf1 (18-181) after HRV 3C protease cleavage to remove the MBP tag, followed by SOURCE 15Q anion exchange and Superdex75 size. exclusion chromatography (GE Healthcare). To obtain a heterodimer of Rac1 (Q61L/P29S, 1-188) and Arf1 (18-181) that were used in the actin polymerization assay, we inserted a heterodimeric GCN4-derived coiled coil (CC) followed by a flexible GGS linker between the MBP-Tev-tag and Rac1 (using the acidic CC) or Arf1 (using the basic CC) (*38*). The MBP-CC-GTPases were expressed and purified individually from BL21(DE3)^{T1R} cells (Sigma), combined in ~1:1 molar ratio to form a heterodimer, treated with Tev to remove the MBP tag, and purified by SOURCE 15S cation exchange and Superdex75 size exclusion chromatography (GE Healthcare).

GST pull-down assays and pyrene-actin polymerization assays used previously established protocols (*37, 38*). Prior to use, Arf1 (alone or in heterodimer with Rac1) was loaded with GDP, GTP (in pull-down) or the non-hydrolyzable GTP analog GMPPNP (in actin polymerization assay) by following a similar protocol used for Rac1 WT, except that we changed the incubation condition to 37°C for 45-60 min

in order to maximize the loading efficiency for Arf1 (*37*). Note that Rac1 (Q61L/P29S, 1-188) is constitutively active and cannot be loaded with GDP under the same conditions, despite various temperature and incubation times that were tested.

Immunoprecipitation (IP)–Mass Spectrometry

To analyze HEM1 and WAVE2 interacting proteins three sets of IPs were done followed by quantitative mass spectrometry. Firstly, from 10^8 cells, an IP was performed with either a rabbit isotype (CST) or WAVE2 antibody (CST) followed by two washes in lysis buffer and two more in detergent-free lysis buffer. Magnetic IP beads were then resuspended in sodium dodecanoate and boiled. The second set of IPs was performed using the WAVE2 antibody in either lysates generated from 5×10^7 WAVE2-deficient Jurkat cells, HEM1-WT-Flag reconstituted cells, or HEM1-M371V-Flag reconstituted cells. Samples were again washed twice in lysis buffer and twice in detergent free lysis buffer and resuspended in sodium dodecanoate and boiled. For the third set of IPs, FLAG was immunoprecipitated from 5×10^7 HEM1-deficient cells, HEM1-WT-Flag reconstituted cells, or HEM1-M371V reconstituted cells. Samples were again washed twice in lysis buffer and twice in detergent free lysis buffer and resuspended in sodium dodecanoate and boiled for 5 min.

Briefly, control/experiment pairs were compared essentially by LC/MS/MS using the affinity enrichment approach with isotope-based quantitation based on post digestion reductive di-methylation and data processing using MaxQuant. (*39-41*) More specifically, to each sample (containing 100 μl 1% sodium dodecanoate), 10 μl of a urea-unfolded solution of non-reduced Hen ovalbumin (about 0.3 picomole) was added. To ensure a controlled pH, 50 μl of 1M Tris (pH 8.0) was added and then 3 μl of 0.4M DTT was added and the sample heated to 50°C for 20 min. After cooling to room temperature, 6 μ of 0.5 M chloroacetamide was added and the samples incubated in the dark for 1 hour, after which 3 μ of beta-mercaptoethanol was added to scavenge remaining chloroacetamide. Next the samples were diluted to 0.1% dodecanoate and 2 μg of trypsin (5 ul, V5113), mixed thoroughly, and incubated overnight at room temperature. Sodium dodecanoate/laurate was removed by adding 50 μl of 10% formic acid, samples were washed three times with 0.5 volumes ethyl acetate, and phase separation was reestablished after vigorous mixing and a short spin at $800 \times g$ (*42*). After extraction, the aqueous fraction was moved to a fresh vial and

a further 200 μl of 0.4% formic acid was added to recover residual sample from the leftover aqueous phase in the original sample vial. This solution was withdrawn and combined with the bulk of each sample. Each sample was dried down briefly with a stream of warm nitrogen gas before being chilled in ice water. Each sample was then applied to STAGE tips and labeled by reductive dimethylation on column essentially as described as protocol C (*40, 42*). After elution, most of each sample was mixed with its pair partner. Light labeling (+28) was used for the control and intermediate (+32) was used for the pull-down samples. To improve the quality of ratio estimation with high background samples from lightly washed pull-downs, the mixed sample was fractionated using a concatenated high pH (pH 10) reversed phase approach as described (*40*). Future applications of high pH fractionation of dimethyl labeled samples such as this might be improved by performing them at slightly lower pH to avoid the potential beta-effects of isotopic forms at higher pH 10. (*41-44*). This effect may have played a role in a small number of declinations by software to make ratio calls in later data analysis.

Data was next collected on an LC/MS/MS system comprising a Thermo nLC-1000 and Thermo Orbitrap Fusion Lumos configured with an EASY-Spray source. The nLC-100 used an A-solvent of 0.1% formic acid and a B-solvent of 93.75% acetonitrile and 0.1% formic acid. From a final 40 μl of sample, 18 μl was injected and loaded at 450 bar onto an EASY-Spray column (50 cm x 75 μm ID, PepMap RSLC C18, 2 μm) and separated at a flow rate of 100 nl/min with a gradient of 5 to 22% in 215 min, followed by a gradient to 32% in 30 min, and then to 95% in 20 min. Parent spectra were collected using the orbit rap with a 120K resolution setting after which ion trap spectra of HCD fragmented targets were collected for up to 5 s. Peptide like mono-isotopic peak detection, 1E3 intensity, 2-7 charge state, and 2 over 2 second dynamic exclusion (20 second duration) were used as filters. Raw data were processed using MaxQuant 1.6.3.3 using a two-channel analysis with re-quantification and otherwise default settings.

Flow cytometry

Cell-surface receptor staining were performed on ice prior to fixation at room temperature for 30 min – 18 hours following fixation/permeabilization. For intracellular staining, cells were fixed and permeabilized with 3% PFA and 100% ice-cold methanol, washed at least three times, and incubated with antibodies for 1-18

hours at room temperature. Flow cytometric data were acquired on a BD Fortessa with 18-color configuration, an LSRII, or a FACS Caliber and analyzed using FlowJo version 9.9.6 or 10.4.2.

Statistical Analysis

All statistical analyses were done in GraphPad Prism 8. * P<0.05, ** P<0.01, *** P<0.001, *** P<0.0001. Differences that did not reach statistical significance are not indicated. For statistical tests performed between normal donors and patient cells (when three or more patients were tested for that assay), a Student's *t*-test assuming unequal variance was performed. For knockdown and inhibitor experiments, where samples were compared between treated and untreated conditions, a Wilcoxon matched-pairs signed-rank test was performed.

Supplementary Text

Patient Narratives

Pt 1.1

Pt 1.1 is an 11-year-old Canadian First Nations female born to non-consanguineous parents. Whole exome sequencing (WES) revealed three regions of absence of heterozygosity with an identity by descent of 0.86%, indicating her parents may be distant cousins. Following an uncomplicated pregnancy and healthy birth, the patient developed chronic rhinorrhea and cough during the first months of life. At 9 months of age, the patient developed a severe upper respiratory tract infection and viral meningitis. At 15 months of age, a *Streptococcus pneumoniae* bacteremia, necrotizing pneumonia with empyema, and meningitis was diagnosed. During this illness pulmonary hypertension, hepatomegaly, and splenomegaly were noted. Two additional bouts of pneumonia with cough, fever, and respiratory distress occurred in the first 2 years of life. She was diagnosed with asthma with nocturnal hypoxia at 15 months, requiring night-time O_2 supplementation inhaler treatment (including fluticasone-salmeterol and albuterol) which provided limited relief of symptoms. Chronic middle ear infection requiring surgery for tympanostomy tubes occurred at 4 years of age.

Progressive worsening of cough, exercise-intolerance and hypoxia resulted in a hospital admission at 6 years of age. Marked splenomegaly (8 cm below the left costal margin), hepatomegaly (3 cm under the right costal margin), diffuse lymphadenopathy, and clubbing were noted at this time on physical

examination. Pulmonary function tests (PFTs) revealed a restrictive lung pattern (forced exhaled volume (FEV)1 = 36% predicted, forced vital capacity (FVC) = 39% predicted, FEV1/FVC = 0.83) and a computerized tomography (CT) scan demonstrated diffuse interstitial and ground-glass infiltrates in all lobes of the lungs. Elevated IgG and IgE levels (23.1 g/l and 2000 IU/ml, respectively) with normal eosinophil counts and IgM and IgA levels were noted. Quantitatively normal numbers of $CD3^+$, $CD4^+$, and $CD8^+$ T-cells and $CD19^+$ B-cells were present and have remained so over years of subsequent testing. A mild quantitative $CD56^+/CD16^+$ NK-cell deficiency (47 cells/μl) was present at this time, which has continued over years of subsequent testing (33-99 cells/μl). Most striking was a marked elevation in the proportions of double-negative $CD3^+$ T cells (11% of $CD3^+$ T cells at 6 years of age before starting steroids and immune suppression for pulmonary disease; range between 3.7-12.6% over subsequent years of testing).

Biopsy of an axillary lymph node demonstrated an encapsulated lymph node with numerous reactive germinal centers and a reactive paracortex but no double-negative T cells (diagnosed as reactive follicular hyperplasia). Lung biopsy of the right middle lobe demonstrated chronic interstitial lung disease with severe and diffuse interstitial pneumonitis of predominantly lymphocytic origin, with increased alveolar macrophages and rare eosinophils and neutrophils. Bronchiolitis, mild pulmonary arterial medial hypertrophy, pleural fibrosis, and hemorrhage were also seen.

A diagnosis of autoimmune lymphoproliferative syndrome (ALPS) or an ALPS-like syndrome with pulmonary involvement was initially considered. A next generation sequencing panel for ALPS and ALPS-related genes, including mutations in CASP8, CASP10, FADD, FAS, FASLG, ITK, KRAS, NRAS, and MAGT1, revealed no genetic mutations in these targets. The patient was started on prednisone (2 mg/kg/day) and sirolimus, resulting in marked improvement in the pulmonary disease, lymphadenopathy, hepatomegaly, and to a lesser degree splenomegaly. Subsequent trials off corticosteroids but with therapeutic plamsa levels of sirolimus resulted in worsening of the pulmonary symptomatology, PFTs, and lung imaging, necessitating periods of corticosteroid dependence to control the lung disease. Eventually the patient was changed to Mycophenolate Mofetil (MMF) for long-term immune suppression (and has been off all corticosteroids for 2 years), resulting in improvement in symptomatology, lymphadenopathy, and hepatosplenomegaly, although PFTs and double-negative T-cell percentages have not normalized.

Subsequent infections have included a *Streptococcus pneumoniae* bacteremia and bursitis and methicillin-resistant *Staphylococcus aureus* skin pustules and hordeolum. There has been no history of herpes simplex virus infections, molluscum, human papilloma virus, or urticaria.

In addition to the patient's immunological deficiency, she also exhibits signs of a mild extra-hematopoietic disease. Anatomically, the patient has pectus carinatum and poor dentition with small, worn-down central and lateral incisors. Echocardiogram demonstrated trivial tricuspid valve deficiency. The contribution of other rare homozygous variants to the patient clinical phenotype cannot be excluded as she has several homozygous variants of unknown clinical significance that segregate with disease (Table S3).

Pt. 2.1

Pt 2.1 is a 16-year-old female born to non-consanguineous parents of Mexican origin. Family history was negative for lymphoproliferation or immune deficiency, but the medical history revealed that she had a brother who died at 2.5 years due to infections and renal disease. The deceased brother had a positive PPD test and received isoniazid for 9 months; no further history is available for this sibling. No tissue was available for genetic screening of this sibling. Pt 2.1 was born healthy at term. At 6 months of age, she experienced more than six episodes of upper respiratory infections and recurrent ear infections a year. Her pulmonary infections were accompanied by wheezing for which she received asthma treatment with inhaled steroids and albuterol. Antibiotics were given during exacerbations. After 2 years of age, she continued to have recurrent pneumonias and was hospitalized once due to this diagnosis. Also, after 2 years of age, she developed failure to thrive with height and weight below the third percentile for each. Multiple sweat tests were performed and were normal. She was diagnosed with celiac disease and selective IgA deficiency during this period of time. Immunology consult evaluation at 8 years of age revealed clubbing of the fingers, and a purulent ear infection. Her immunologic evaluation showed high IgG levels and undetectable IgA and IgM. T, B, and NK cell numbers were within normal ranges, but NK cell function was decreased. The patient has had recurrent lymphadenopathy and splenomegaly. However, the percentage of $\alpha\beta$ double-negative T cells was below 2%, and the rest of the ALPS evaluation was negative. A chest CT scan revealed peribronchial thickening and bronchiectasis as well as hilar adenopathy. In consideration of her chronic pulmonary symptoms and bronchiectasis, she was started on immunoglobulin (Ig)

replacement and prophylactic treatment with azithromycin. The patient has no history of herpes simplex virus (HSV), molluscum, warts, or urticaria, and acute infection by cytomegalovirus (CMV) or Epstein–Barr virus (EBV) infection. She had one episode of cellulitis post pneumococcal vaccination. The patient has no dysmorphic features and no learning disabilities have been detected. Recently, at 15 years of age, Patient 2.1 had an episode of acute abdominal pain during which she was diagnosed with acute cholecystitis and cholelithiasis requiring uncomplicated cholecystectomy.

Pt. 2.2

Pt 2.2 is the younger sibling of Pt 2.1 and is currently 10 years old. He was first evaluated at 2 years of age because of a history of recurrent ear infections, which began at 12 months of age and recurrent fevers and two prior hospitalizations due to fever with undetermined diagnoses. At the time, he had elevated levels of IgG (1879 mg/dl), IgA (179 mg/dl) and IgM (151 mg/dl). Lymphocyte phenotyping showed increased B cells. At 3 years of age, he had fever and diffuse lymphadenopathy of the cervical, mediastinal, and mesenteric lymph nodes accompanied by hepato-splenomegaly (Supplemental images C). A biopsy of a cervical lymph node performed during this hospitalization showed reactive follicles with subcapsular sinus histiocytosis and emperipolesis suggestive of Rosai–Dorfman disease. Genetic testing for ALPS was negative, and double-negative T cells were not increased. During the same hospitalization, he was noted to have nephrotic range proteinuria and hematuria. In the context of this nephrotic syndrome, a biopsy was performed and showed glomerulonephritis with deposition of immune complexes in a subendothelial and mesangial pattern. The biopsy findings were compatible with lupus nephritis class IV-V but the patient did not fulfill other systemic lupus erythematosus (SLE) criteria at the time. In particular, antinuclear antibody (ANA) and anti-DNA auto antibodies were negative. He was started on steroids and MMF. He continued to have multiple episodes of respiratory infections, including condensing pneumonias and severe, purulent ear infections and his renal disease seemed to be exacerbated by these infections. A chest CT scan obtained in between pulmonary infections revealed bilateral ground glass opacities with no bronchiectasis (Supplemental images). At 7 years of age, he had an exacerbation of the nephrotic syndrome requiring pulsed steroids and initiation of rituximab. After treatment with rituximab, he was also started on subcutaneous Ig infusions to control recurrent infections. His renal disease has been partially controlled

with MMF and rituximab but appears exacerbated by ongoing infections. Despite Ig replacement and antibiotic prophylaxis, he continues to have recurrent episodes of infection, including multiple episodes of pneumonia. One event was associated with pneumococcal bacteremia. He has recently had a pleural effusion. He also continues to have recurrent and persistent otitis media. Between pulmonary infections, he has chronic cough and wheezing. He was diagnosed with asthma at 7 years of age and started on inhaled steroids and bronchodilators, which has led to only partial control of symptoms. After the first episode of lymphadenopathy, he has had multiple exacerbations of lymph node enlargement and hepatosplenomegaly, approximately once a year. During these episodes, he shows enlargement of cervical, mediastinal, mesenteric and inguinal lymph nodes (Supplemental Figure S1A). Multiple biopsies performed during these episodes show reactive follicular enlargement and have ruled out malignancy. Rosai–Dorfman disease has been identified twice in cervical lymph node biopsies. The most recent chest CT scan shows persistence of supraclavicular adenopathy, mediastinal lymph node enlargement, as well as ground-glass and consolidative opacities within the right upper and lower lung lobes. The patient has no history of HSV, molluscum, warts or urticaria, and acute infection by CMV or EBV has not been observed. He has no dysmorphic features; he has problems in school apparently stemming from multiple absences due to his recurrent and extended periods of medical absence.

Pt 3.1

Patient 3.1 is 10-year-old male born to healthy first-degree cousins in the United Arab Emirates. Whole exome sequencing revealed that the patient has eight regions of absence of heterozygosity with an identity by descent of 4.6%, confirming that parents were related. Though born to healthy parents, the patient had three elder brothers that all died at approximately 3 months of age from fever and organ failure indicative of sepsis along with dysregulated inflammation resembling hemophagic lymphohistiocytosis (HLH). At birth, the patient exhibited jaundice and required an extended hospital stay. At 13 months of age, he was hospitalized for invasive and disseminated HSV1 infection, manifesting with muco-cutaneous lesions, hepatitis, and encephalitis (with epilepsy). He required a 4-week hospitalization and anti-seizure therapy due to herpetic meningo-encephalitis. Long-term consequences of the infection included developmental delay and sensorineural hearing loss and lack of speech. At 18 months of age, the patient

developed sudden hearing loss. His subsequent clinical history includes several instances of high fever and splenomegaly requiring hospitalization and administration of antibiotics with blood cultures testing positive for *Pseudomonas aeruginosa*, as-well-as persistent asthma, allergic rhinitis, and allergies (anaphylaxis) to food (shellfish). Additional infections include molluscum contagiosum lesions in the upper chest and head at 7 years, mucoid otitis media at 9 years, and roseola infantum at 10 years of age. Despite normal serum Ig levels at the time of testing, the patient had poor pneumococcal-specific antibody titer following polysaccharide pneumococcal vaccine administration and developed autoimmune thrombocytopenia following MMR vaccination. In addition to the immunological abnormalities, the patient is obese and, along with his elder sister, displays bleeding tendencies with gum and skin bruising. He has an abnormal platelet function test, low Factor XII level, and prolonged partial thromboplastin time. The family history is significant for easy fractures and recurrent fever in the oldest brother and temporal arachnoid cysts with history of craniotomy, mental developmental delay (autism-like), and a ganglion cyst excision (right wrist) in another brother. All siblings have significant dentition problems with retention of primary teeth. The syndromic symptoms are suggestive of one or more additional genetic diseases within the family. Supporting this likelihood, the patient has several homozygous variants of unknown significance, including in proteins known to be important for bone development and cognitive function (Table S3).

Pt 4.1

Patient 4.1 is a 2.5-year-old female born to non-consanguineous parents from north-Africa with two healthy sisters. She had features of a syndromic disease at birth, including intracerebral ventricular dilatation (unilateral) and ventricular heterotopia, liver calcification (liver hamartoma), kidney dilatation, cardiomegaly, and muscular ventricular septal defect with dilatation of the ascending aorta. Following birth, the patient developed aortic bicuspidia, and had oral feeding issues requiring a gastric tube. At approximately 1 year of age, the patient developed pulmonary symptoms with alveolar interstitial syndrome and pancytopenia. However, no bacterial or viral infection was detected. One month later, she was admitted to the hospital for persistent fever, splenomegaly, hyperferritinemia, hypofibrinogenemia, hypertriglyceridemia, and an EBV viral load of 3.8 log copies/ml. The patient was subsequently diagnosed with EBV-driven HLH. No defect in T cell degranulation, perforin expression, or hair color was detected.

She was treated with corticosteroids, cyclosporine, and two rounds of rituximab. Following an initial recovery, the EBV viral load again increased after 8 months to 3.6 log copies/ml with no detectable anti-EBNA IgG, indicating a lack of seroconversion and poor specific antibody production. She developed hepatosplenomegaly at 1 year of age, which continues to persist. The patient has also had recurrent otitis media and pneumonia with the development of bronchiectasis and recurrent asthma.

Figure S1.

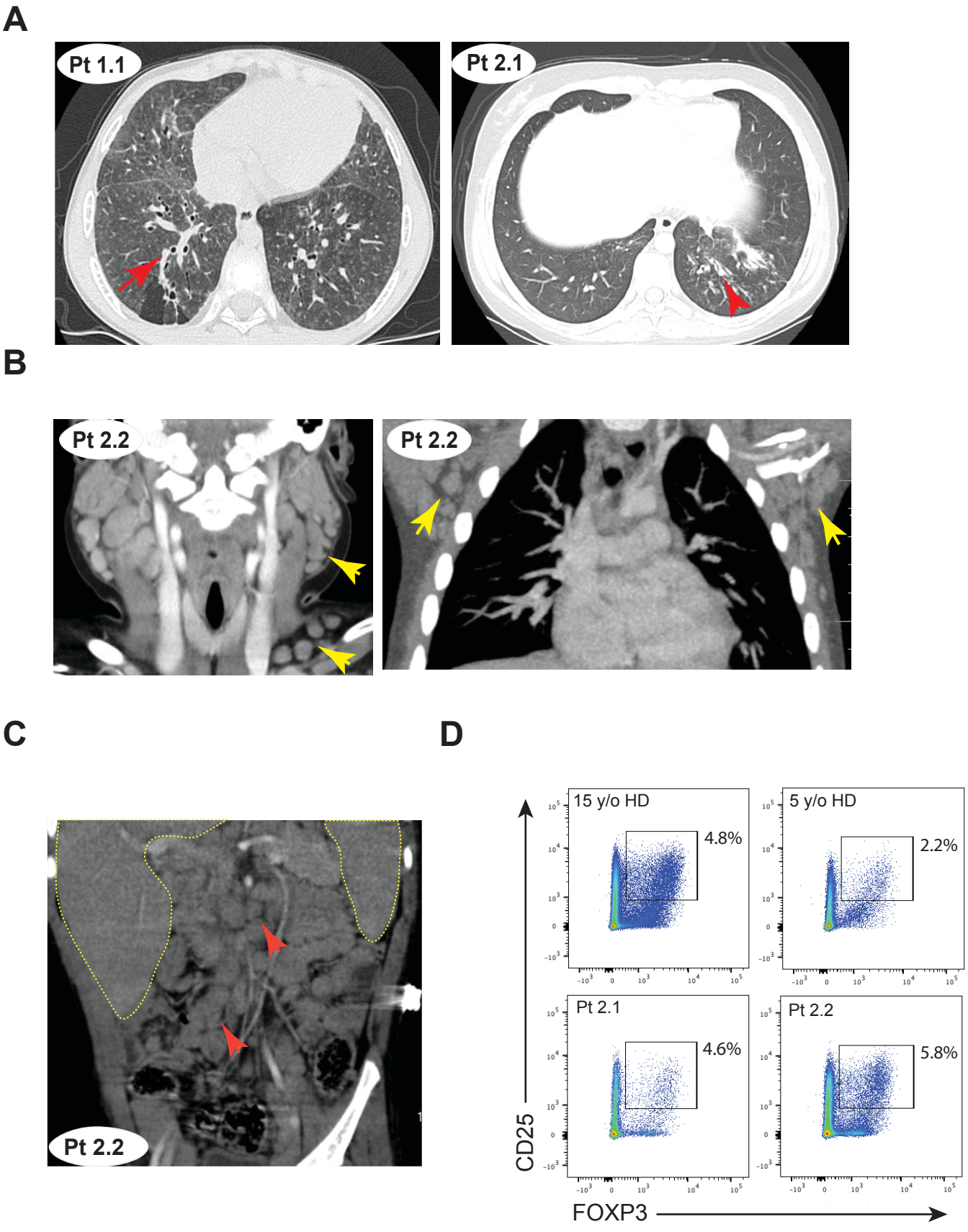
A
Pt 1.1
Pt 2.1
B
Pt 2.2
Pt 2.2
C
Pt 2.2
D
15 y/o HD
4.8%
5 y/o HD
2.2%
Pt 2.1
4.6%
Pt 2.2
5.8%
CD25
FOXP3

Figure S1. Patients have immunodeficiency, immune hyperactivity and lymphadenopathy, and normal T reg cell numbers. (**A**) Chest computerized tomography (CT) scans showing bronchiectasis in Patients 1.1 and 2.1 indicated by red arrows. (**B**) CT scans showing lymphadenopathy in Pt 2.2 (yellow arrows). (**C**) CT scan of Patient 2.2 demonstrating hepatosplenomegaly (yellow outlines) and mediastinal lymphadenopathy (red arrows). (**D**) Percentage of $CD4^+$ T regulatory cells expressing CD25 and FOXP3 in Pts 2.1 and 2.2 and age-matched healthy donors (HD).

Figure S2.

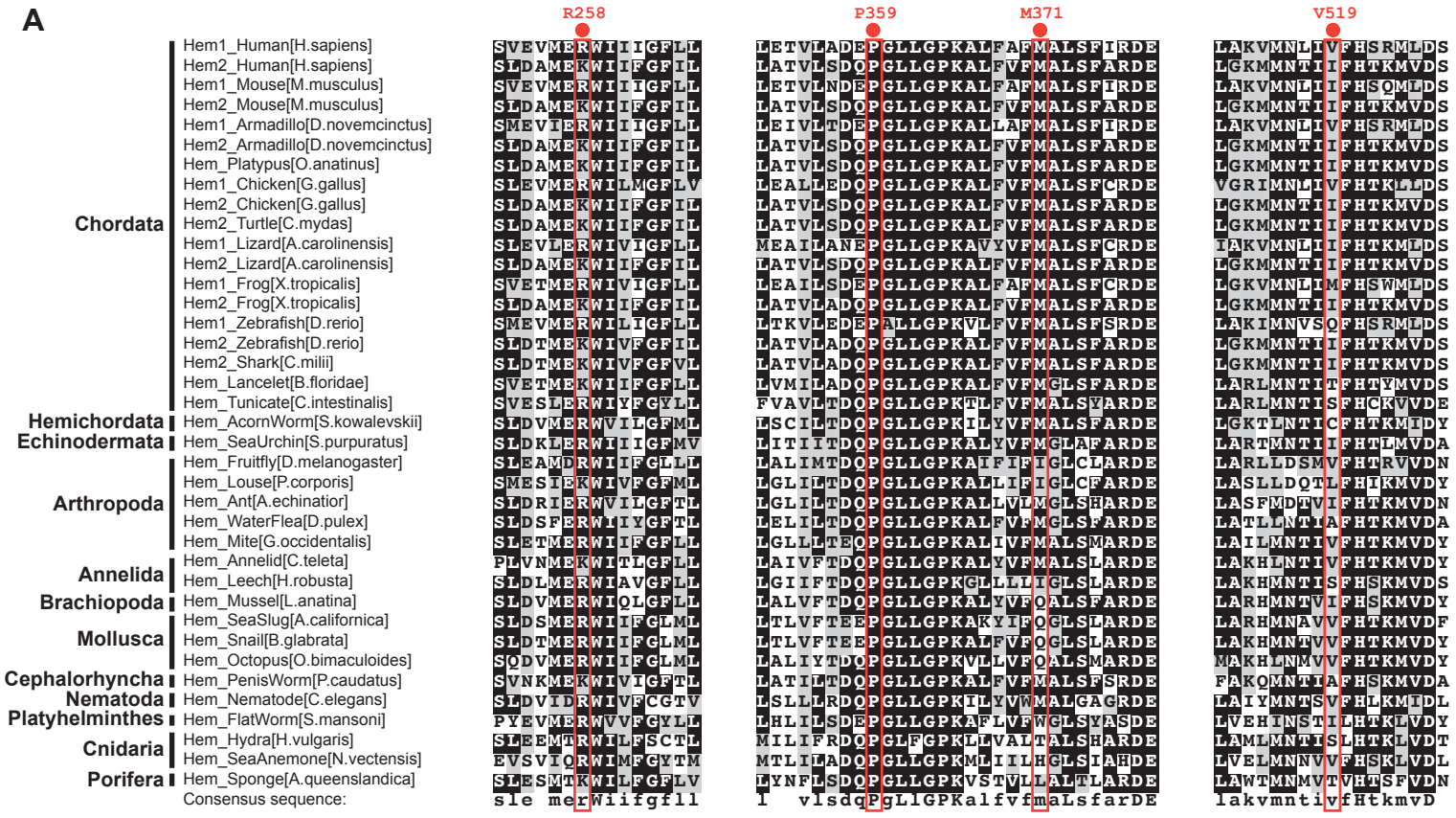

B

	R258L	P359L	M371V	V519L
SIFT	0	0	0.03	0.07
PolyPhen	0.104	0.999	0.098	0.037
CADD	32	27	24	20.6

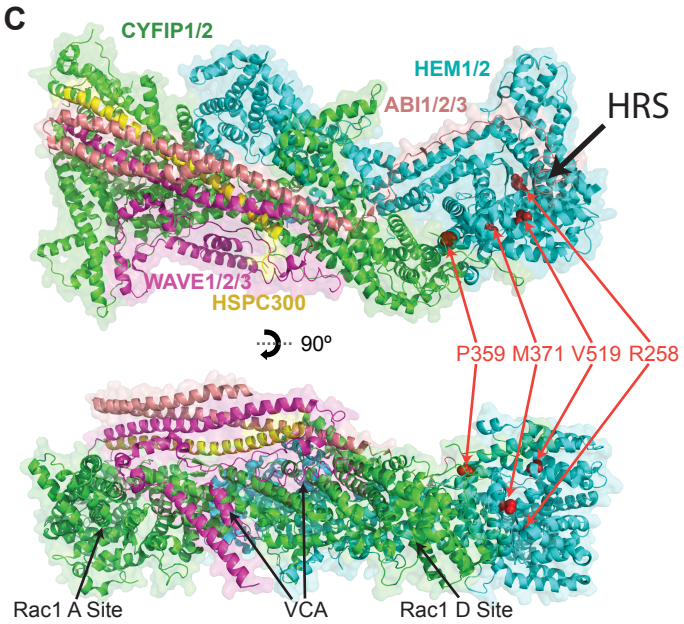

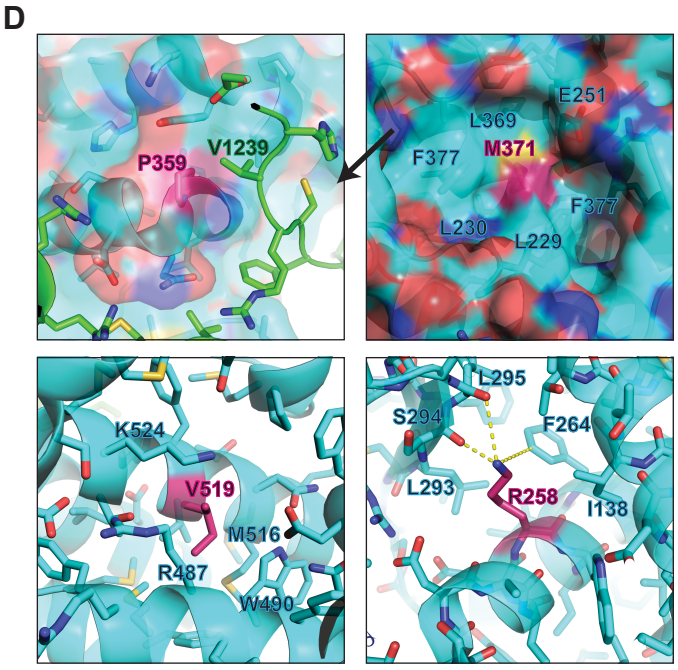

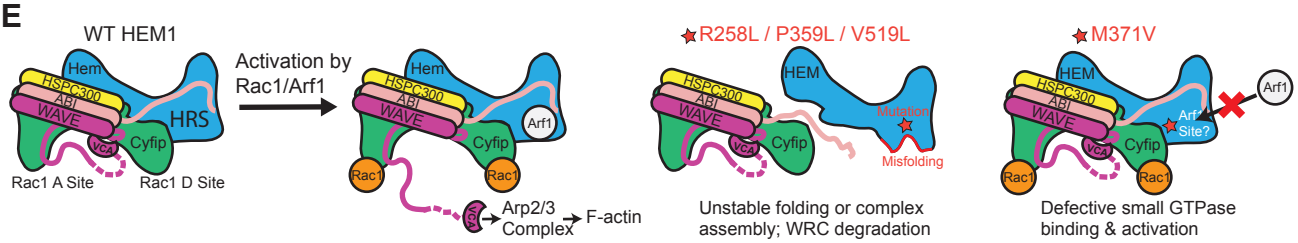

Figure S2. Patient-derived *NCKAP1L* mutations fall within conserved regions and have detrimental effects on the structure and function of the WRC. (**A**) Multiple sequence alignment of *NCKAP1L* (HEM1) and *NCKAP1* (HEM2) from various animal species, with locations of patient-derived mutations indicated in red. Black shows exactly conserved residues and gray shows chemically conserved residues. (**B**) Deleterious predictions of various algorithms for each of the patient mutations. Red numbers indicate that the patient mutation is above the cut-off to be considered deleterious by the indicated program. (**C**) Location of the patient variants in HEM1 in relationship to the overall structure of the WRC. (**D**) Local structures of HEM1 patient mutations. Residues (shown in sticks) in close contact with the mutated amino acids (in purple) are indicated to illustrate lost contacts or structural alterations upon substitution. (**E**) Schematic showing the impacts of different HEM1 mutations on the structure and function of the WRC during activation.

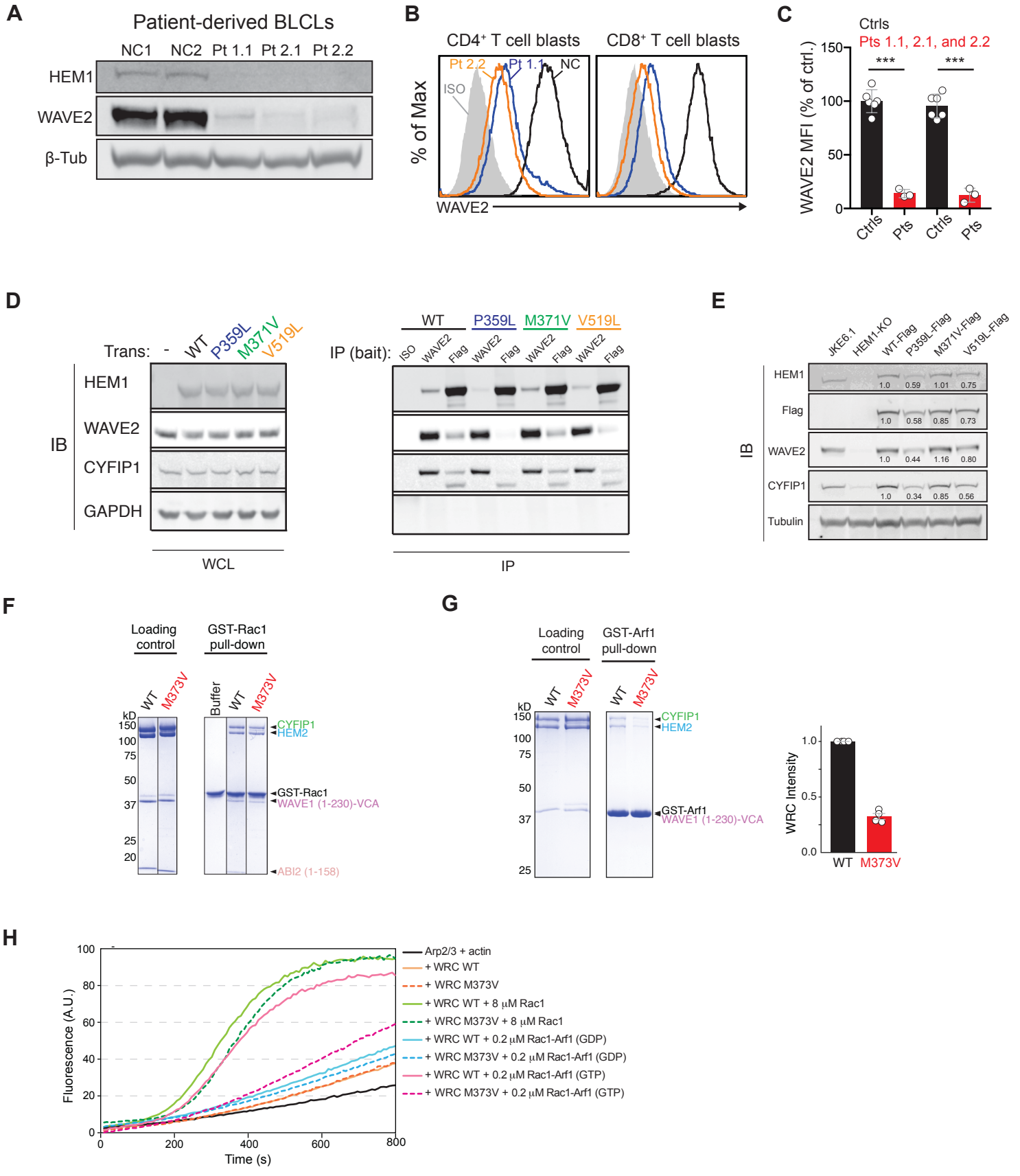
A
Patient-derived BLCLs
NC1 NC2 Pt 1.1 Pt 2.1 Pt 2.2
HEM1
WAVE2
β-Tub
B
CD4⁺ T cell blasts
CD8⁺ T cell blasts
Pt 2.2
Pt 1.1
NC
ISO
% of Max
WAVE2
C
Ctrls
Pts 1.1, 2.1, and 2.2
***
***
WAVE2 MFI (% of ctrl.)
150
100
50
0
Ctrls
Pts
Ctrls
Pts
D
Trans: - WT P359L M371V V519L
IP (bait): WT P359L M371V V519L
ISO WAVE2 Flag WAVE2 Flag WAVE2 Flag WAVE2 Flag
IB
HEM1
WAVE2
CYFIP1
GAPDH
WCL
IP
E
JKE6.1
HEM1-KO
WT-Flag
P359L-Flag
M371V-Flag
V519L-Flag
IB
HEM1
Flag
WAVE2
CYFIP1
Tubulin
1.0 0.59 1.01 0.75
1.0 0.58 0.85 0.73
1.0 0.44 1.16 0.80
1.0 0.34 0.85 0.56
F
Loading control
GST-Rac1 pull-down
WT
M373V
Buffer
kD
150
100
75
50
37
25
20
CYFIP1
HEM2
GST-Rac1
WAVE1 (1-230)-VCA
ABI2 (1-158)
G
Loading control
GST-Arf1 pull-down
WT
M373V
kD
150
100
75
50
37
25
CYFIP1
HEM2
GST-Arf1
WAVE1 (1-230)-VCA
WRC Intensity
1.0
0.5
0.0
WT
M373V
H
Fluorescence (A.U.)
100
80
60
40
20
0
0
200
400
600
800
Time (s)
Arp2/3 + actin
+ WRC WT
+ WRC M373V
+ WRC WT + 8 μM Rac1
+ WRC M373V + 8 μM Rac1
+ WRC WT + 0.2 μM Rac1-Arf1 (GDP)
+ WRC M373V + 0.2 μM Rac1-Arf1 (GDP)
+ WRC WT + 0.2 μM Rac1-Arf1 (GTP)
+ WRC M373V + 0.2 μM Rac1-Arf1 (GTP)

Figure S3

Figure S3. Patient-derived HEM1 variants destabilize the WRC or impair Arf1 binding and activation. (**A**) Immunoblot of WRC components HEM1 and WAVE2 in lysates derived from Epstein–Barr virus (EBV)-transformed B-lymphoblastoid cell lines (BLCL) from normal controls (NC) or Pts. Loading control: beta tubulin (β-Tub). (**B**) Representative flow cytometry histograms showing intracellular WAVE2 expression in $CD4^+$ or $CD8^+$ T cell blasts derived from Pt or NC PBMCs. Isotype (Iso) control peak is shown in gray. (**C**) Quantification of WAVE2 mean fluorescence intensity (MFI) in patient and control $CD4^+$ or $CD8^+$ T cell blasts as in (B). (**D**) Immunoblot showing WRC components HEM1, WAVE2, and CYFIP1 immunoprecipitated by the indicated FLAG-tagged HEM1 proteins (WT or patient variant), by WAVE2, or by an isotype control antibody in a 293 overexpression system. GAPDH: loading control. WCL: whole cell lysate. IB: immunoblot staining. IP: immunoprecipitate. (**E**) Immunoblot of WRC components, FLAG, or tubulin loading control using lysates from JKE6.1 cells, a single cell JKE6.1 clone deficient for HEM1 stably reconstituted with Flag-tagged wild-type (WT) or amino acid substitution HEM1 protein. Densitometry values are listed under each lane. (**F**) Coomassie blue-stained SDS–PAGE gels showing GST-Rac1 (Q61L/P29S) pull-down assay of recombinantly purified WRC containing either WT or M373V HEM2 and WAVE1 (1-230)-VCA. Position of CYFIP1, HEM2, GST-Rac1, WAVE1, and Abi2 are shown. Loading controls contain 4 pmol of the WRC. (**G**) Coomassie blue-stained SDS–PAGE gels showing GST-Arf1 pull-down of the purified WRC used in (F) and (H) in the presence of Rac1 (Q61L/P29S). Lanes were from the same gel. Position of the GST-Arf1 protein is shown. (Right) Quantification of the retained WRC across four repetitions (mean ± SEM). (**H**) Pyrene-actin polymerization assay with WRC230VCA containing HEM2 WT or M373V, with or without activation by a Rac1-Arf1 heterodimer pre-loaded with GMPPNP (See Methods for details). As a control, polymerization with Rac1 was efficient for both WT- and M373V-HEM2 containing WRC.

Figure S4.

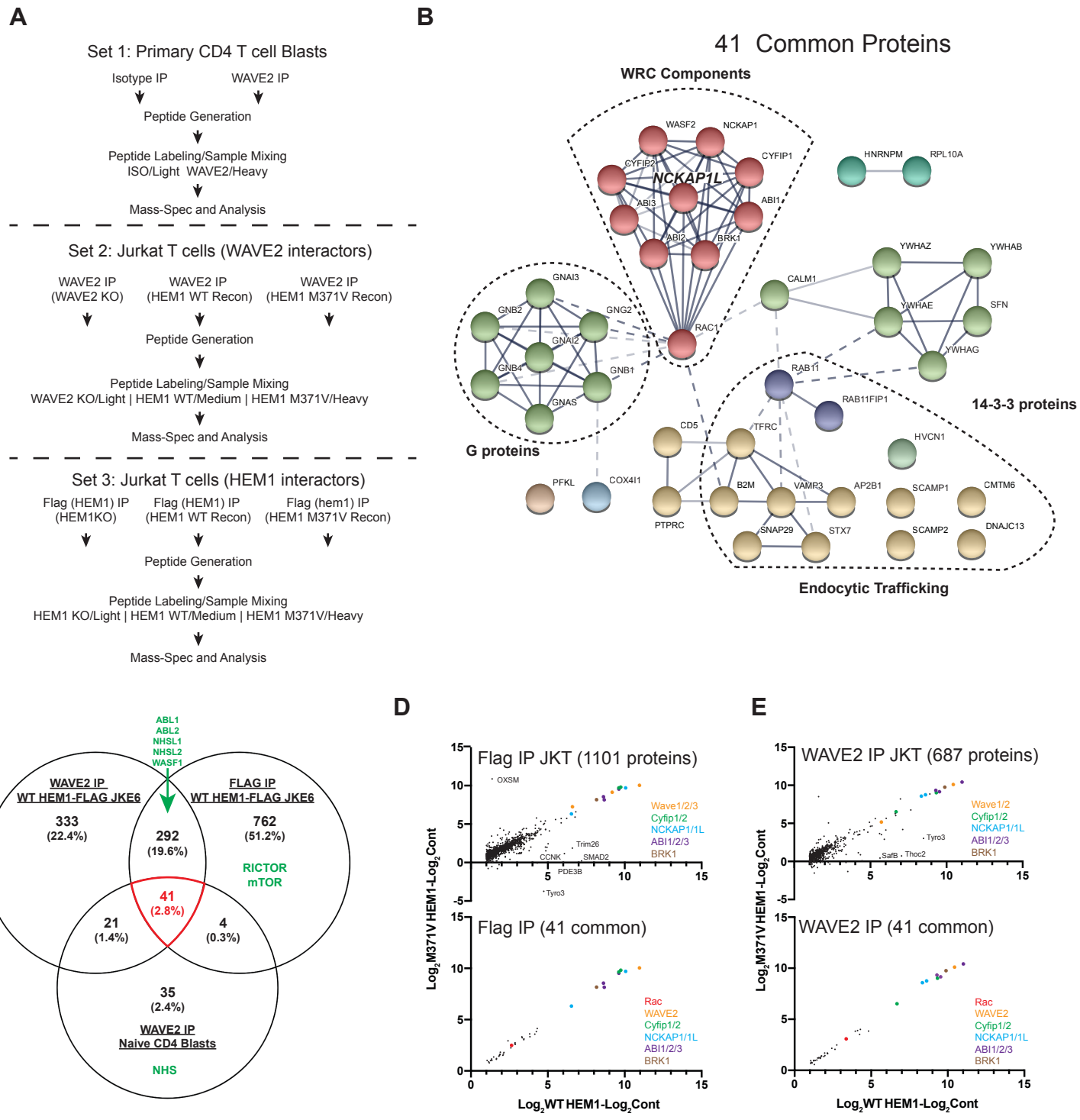
A
Set 1: Primary CD4 T cell Blasts
Isotype IP
WAVE2 IP
Peptide Generation
Peptide Labeling/Sample Mixing
ISO/Light WAVE2/Heavy
Mass-Spec and Analysis
Set 2: Jurkat T cells (WAVE2 interactors)
WAVE2 IP (WAVE2 KO)
WAVE2 IP (HEM1 WT Recon)
WAVE2 IP (HEM1 M371V Recon)
Peptide Generation
Peptide Labeling/Sample Mixing
WAVE2 KO/Light | HEM1 WT/Medium | HEM1 M371V/Heavy
Mass-Spec and Analysis
Set 3: Jurkat T cells (HEM1 interactors)
Flag (HEM1) IP (HEM1KO)
Flag (HEM1) IP (HEM1 WT Recon)
Flag (hem1) IP (HEM1 M371V Recon)
Peptide Generation
Peptide Labeling/Sample Mixing
HEM1 KO/Light | HEM1 WT/Medium | HEM1 M371V/Heavy
Mass-Spec and Analysis
B
41 Common Proteins
WRC Components
WASF2
NCKAP1
CYFIP2
CYFIP1
NCKAP1L
ABI3
ABI1
ABI2
BRK1
RAC1
HNRNPM
RPL10A
YWHAZ
YWHAB
CALM1
YWHAE
SFN
YWHAG
GNAI3
GNB2
GNG2
GNAI2
GNB4
GNB1
GNAS
G proteins
14-3-3 proteins
RAB11
RAB11FIP1
CD5
TFRC
HVCN1
PFKL
COX4I1
B2M
VAMP3
AP2B1
SCAMP1
CMTM6
PTPRC
SNAP29
STX7
SCAMP2
DNAJC13
Endocytic Trafficking
C
ABL1
ABL2
NHSL1
NHSL2
WASF1
WAVE2 IP WT HEM1-FLAG JKE6
FLAG IP WT HEM1-FLAG JKE6
333 (22.4%)
292 (19.6%)
762 (51.2%)
RICTOR mTOR
41 (2.8%)
21 (1.4%)
4 (0.3%)
35 (2.4%)
WAVE2 IP Naive CD4 Blasts
NHS
D
Flag IP JKT (1101 proteins)
OXSM
Trim26
CCNK
SMAD2
PDE3B
Tyro3
Wave1/2/3
Cyfip1/2
NCKAP1/1L
ABI1/2/3
BRK1
Flag IP (41 common)
Rac
WAVE2
Cyfip1/2
NCKAP1/1L
ABI1/2/3
BRK1
Log2M371V HEM1-Log2Cont
Log2WT HEM1-Log2Cont
E
WAVE2 IP JKT (687 proteins)
Tyro3
SafB
Thoc2
Wave1/2
Cyfip1/2
NCKAP1/1L
ABI1/2/3
BRK1
WAVE2 IP (41 common)
Rac
WAVE2
Cyfip1/2
NCKAP1/1L
ABI1/2/3
BRK1
Log2M371V HEM1-Log2Cont
Log2WT HEM1-Log2Cont

Figure S4. IP–MS of WAVE2 and Hem1 show conserved set of interactors in addition to components of the WRC. (**A**) Workflow of immunoprecipitation-mass spectrometry experiments. (**B**) STRING Protein-Protein Interaction mapping on the 41 proteins identified in all three immunoprecipitations. (**C**) Venn Diagram showing number of commonly identified and unique proteins. Proteins that are known to interact with the WRC but were not identified in all three experimental setups are shown in green. (**D**) Relative abundance of proteins identified by quantitative mass-spec in the Flag IP in Jurkat T (JKT) cells from the WT and M371V HEM1 variants (top) or limiting the comparison to those proteins identified in all three IP-mass spec experiments (bottom). (**E**) Relative abundance of proteins identified by quantitative mass-spec in the Wave2 IP in JKT cells from the WT and M371V HEM1 variants (top) or limiting the comparison to those proteins identified in all three IP–MS experiments (bottom).

Figure S5.

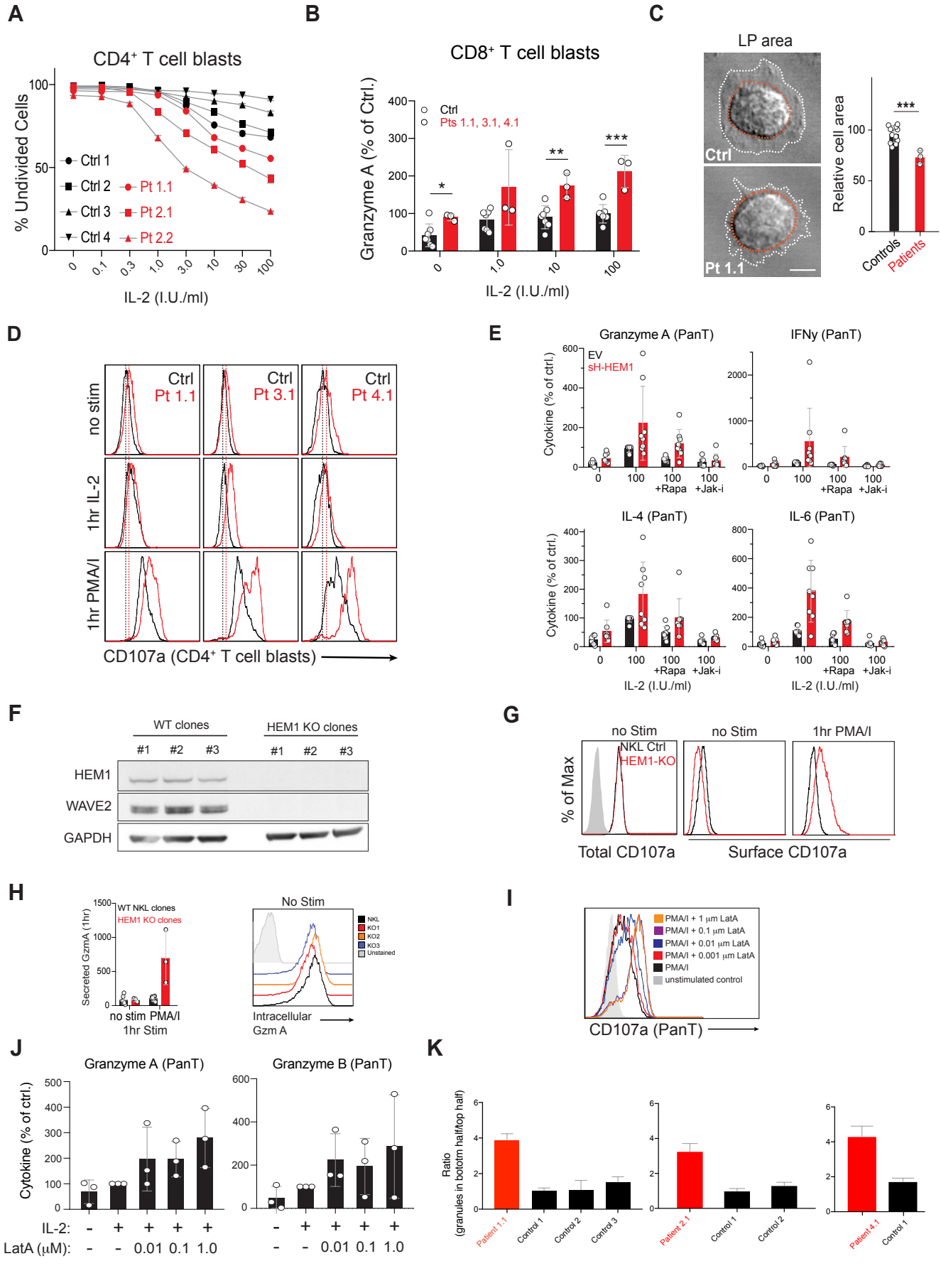
A
CD4⁺ T cell blasts
% Undivided Cells
Ctrl 1
Ctrl 2
Ctrl 3
Ctrl 4
Pt 1.1
Pt 2.1
Pt 2.2
IL-2 (I.U./ml)
B
CD8⁺ T cell blasts
Granzyme A (% of Ctrl.)
Ctrl
Pts 1.1, 3.1, 4.1
IL-2 (I.U./ml)
C
LP area
Ctrl
Pt 1.1
Relative cell area
Controls
Patients
D
no stim
1hr IL-2
1hr PMA/I
Ctrl
Pt 1.1
Pt 3.1
Pt 4.1
CD107a (CD4⁺ T cell blasts)
E
Granzyme A (PanT)
IFNγ (PanT)
IL-4 (PanT)
IL-6 (PanT)
EV
sH-HEM1
Cytokine (% of ctrl.)
+Rapa
+Jak-i
IL-2 (I.U./ml)
F
WT clones
HEM1 KO clones
HEM1
WAVE2
GAPDH
G
no Stim
1hr PMA/I
NKL Ctrl
HEM1-KO
% of Max
Total CD107a
Surface CD107a
H
WT NKL clones
HEM1 KO clones
Secreted GzmA (1hr)
no stim
PMA/I
1hr Stim
No Stim
NKL
KO1
KO2
KO3
Unstained
Intracellular
Gzm A
I
PMA/I + 1 μm LatA
PMA/I + 0.1 μm LatA
PMA/I + 0.01 μm LatA
PMA/I + 0.001 μm LatA
PMA/I
unstimulated control
CD107a (PanT)
J
Granzyme A (PanT)
Granzyme B (PanT)
Cytokine (% of ctrl.)
IL-2:
LatA (μM):
K
Ratio
(granules in bottom half/top half)
Patient 1.1
Control 1
Control 2
Control 3
Patient 2.1
Control 1
Control 2
Patient 4.1
Control 1

Figure S5. Patient-derived T cells and HEM1-deficient T cells show cytokine hypersecretion, abnormal lamellipodia, and increased degranulation. (**A**) Percent of rested T cell blasts remaining in the undivided peak following restimulation as in Figure 2B. (**B**) Soluble granzyme A release from rested control (Ctrl) or patient (Pt) $CD8^+$ T cell blasts following 18-hour stimulation with the indicated doses of IL-2. I.U.: international units; (**C**) Representative photomicrographs of a $CD4^+$ T cell blast from either a Ctrl or Pt 1.1 spreading on stimulatory coverslips as in Figure 2C. The lamellipodial (LP) region is highlighted between the plasma membrane (white) and nucleus (red) (left). Scale bar: 4 μm. The cell area is quantified as averages across multiple experiments (right). (**D**) Flow cytometry histograms of surface CD107a on control (Ctrl) or patient (Pt) purified CD4+ T cell blasts following no stimulation (no stim) or 1-hour stimulation with either 100 I.U./ml IL-2 or 10 ng/ml PMA/I. Dotted lines indicate the mean fluorescence intensity of the unstimulated control or patient samples. (**E**) Soluble release of cytokines from normal control T cell blasts transduced with either empty vector (EV) or shRNA against HEM1 (sH-HEM1) following 18-hour stimulation with the indicated amount of IL-2, with or without addition of rapamycin (rapa) or a pan Jak inhibitor (Jak-i). Each dot represents a different control donor performed in triplicate technical replicates. (**F**) Immunoblot showing HEM1 and WAVE2 in three wild-type (WT) and three HEM1 CRISPR-RNP derived knockout (KO) clones. (**G**) Representative histograms showing intracellular (total) and cell surface CD107a levels on either normal or HEM1 knockout (KO) NKL cells following stimulation with PMA/I for 1 hour. (**H**) Secretion of granzyme A from WT and HEM1-KO lines following a 1-hour stimulation with PMA/I (left). Baseline levels of intracellular granzyme A in WT and KO NKL cell lines (right). (**I**) Surface CD107a on purified T cell blasts following 1-hour PMA/I stimulation and the indicated dose of latrunculin A (LatA). (**J**) Soluble granzymes released from purified control T cell blasts treated with 100 I.U./ml IL-2 and the indicated amount of LatA for 18 hours. Data represent three independent experiments. (**K**) Three independent experiments quantifying the ratio of perforin granule location (bottom half/top half) in patients or control CD8+ T cell blasts by confocal imaging as in Fig. 2E (mean ± SD). Statistical analyses for (B) and (C) were performed using a *t*-test without assuming equal variance. [$*P \leq 0.05$, $**P \leq 0.01$, $***P \leq 0.001$.]

Figure S6.

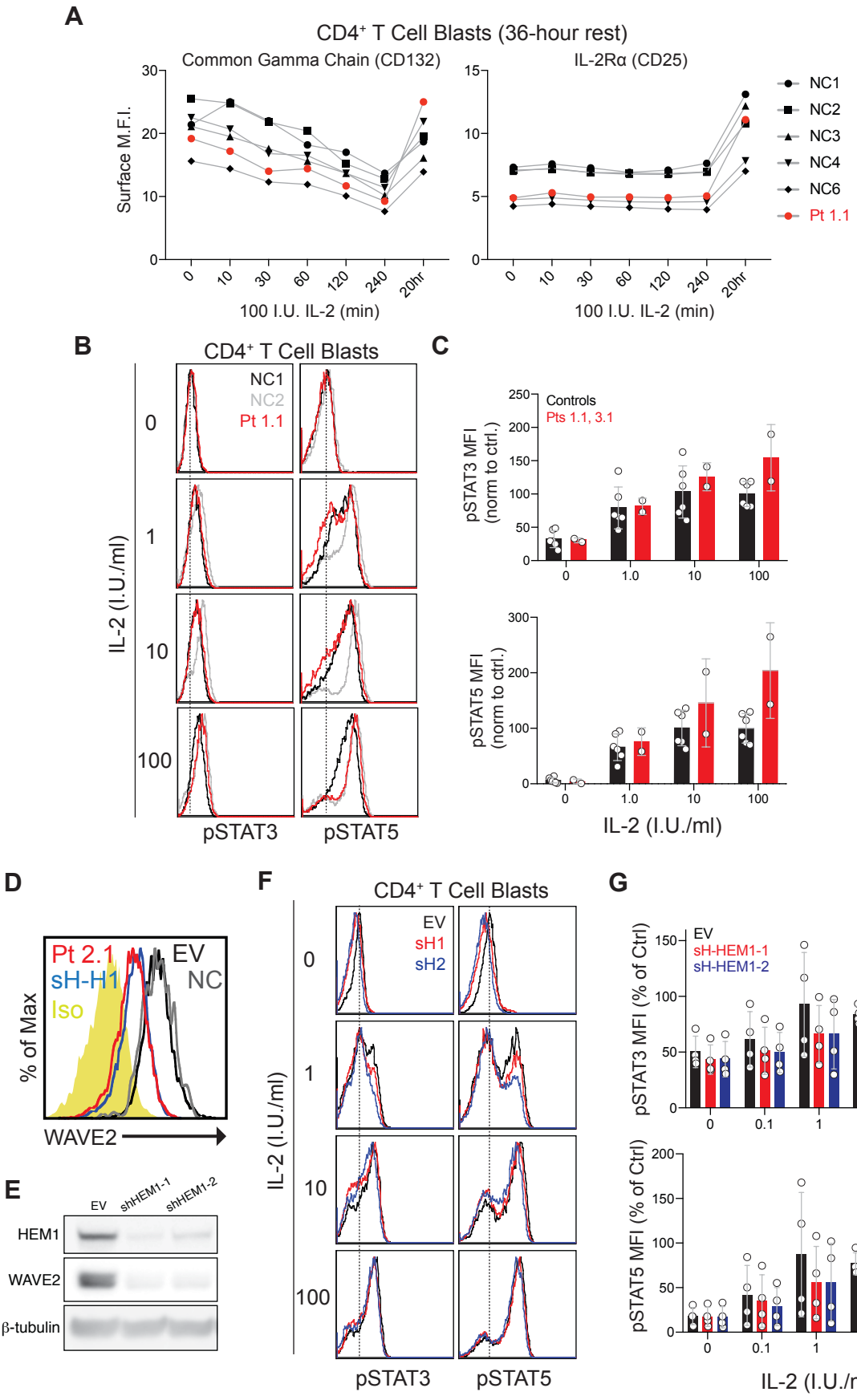
A
CD4⁺ T Cell Blasts (36-hour rest)
Common Gamma Chain (CD132)
IL-2Rα (CD25)
Surface M.F.I.
100 I.U. IL-2 (min)
NC1
NC2
NC3
NC4
NC6
Pt 1.1
B
CD4⁺ T Cell Blasts
IL-2 (I.U./ml)
pSTAT3
pSTAT5
C
Controls
Pts 1.1, 3.1
pSTAT3 MFI (norm to ctrl.)
pSTAT5 MFI (norm to ctrl.)
IL-2 (I.U./ml)
D
Pt 2.1
sH-H1
Iso
EV
NC
% of Max
WAVE2
E
EV
shHEM1-1
shHEM1-2
HEM1
WAVE2
β-tubulin
F
CD4⁺ T Cell Blasts
EV
sH1
sH2
IL-2 (I.U./ml)
pSTAT3
pSTAT5
G
EV
sH-HEM1-1
sH-HEM1-2
pSTAT3 MFI (% of Ctrl)
pSTAT5 MFI (% of Ctrl)
IL-2 (I.U./ml)

Figure S6. HEM1-deficiency does not affect IL-2 receptor surface expression or proximal STAT kinase activation. (**A**) CD132 and CD25 surface expression following addition of 100 I.U./ml human IL-2 to patient and control CD4+ T cell blasts following a 36-hour rest without IL-2. (**B**) Representative flow plots and (**C**) combined mean fluorescence intensity (MFI) quantification from two independent experiments of Pt 1.1 and Pt 3.1 CD4+ T cell blasts compared to normal control (NC) showing induction of STAT3 and STAT5 phosphorylation after a 10-min stimulation with the indicated amount of IL-2. (**D**) Flow cytometry histogram showing intracellular WAVE2 levels in $CD4^+$ T cells from a normal control (NC2) or Pt. 2.2, or normal $CD4^+$ T cells transduced with empty lentivirus vector (EV) or HEM1-shRNA (sh-H1). (**E**) Immunoblot showing HEM1 knockdown efficiency by two different HEM1-targeting shRNA vectors (shHEM1-1 and shHEM1-2) compared to EV. (**F**) Representative flow plots and (**G**) combined MFI quantification from four independent experiments showing induction of STAT3 and STAT5 phosphorylation after a 10-min stimulation with the indicated amount of IL-2 in CD4+ T cell blasts derived from normal donors and transduced with the EV or sh HEM1 vectors shown in (E). Data represent at least three independent experiments.

Figure S7.

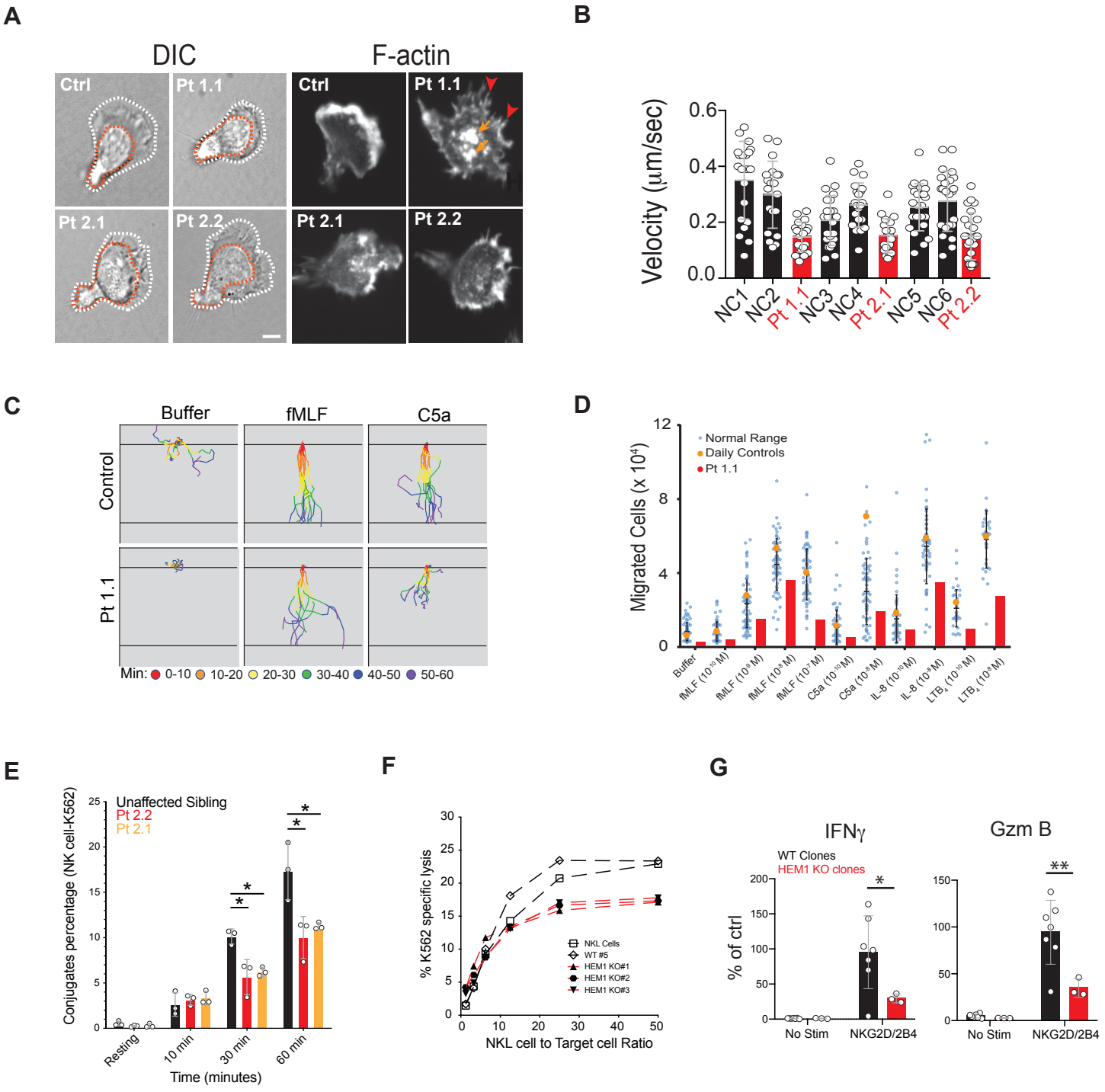
A
DIC
F-actin
Ctrl
Pt 1.1
Pt 2.1
Pt 2.2
B
Velocity (µm/sec)
0.6
0.4
0.2
0.0
NC1
NC2
Pt 1.1
NC3
NC4
Pt 2.1
NC5
NC6
Pt 2.2
C
Buffer
fMLF
C5a
Control
Pt 1.1
Min: 0-10 10-20 20-30 30-40 40-50 50-60
D
Migrated Cells (x 10⁴)
12
8
4
0
Normal Range
Daily Controls
Pt 1.1
Buffer
fMLF (10⁻¹⁰ M)
fMLF (10⁻⁹ M)
fMLF (10⁻⁸ M)
fMLF (10⁻⁷ M)
C5a (10⁻¹⁰ M)
C5a (10⁻⁹ M)
IL-8 (10⁻¹⁰ M)
IL-8 (10⁻⁹ M)
LTB4 (10⁻¹⁰ M)
LTB4 (10⁻⁹ M)
E
Conjugates percentage (NK cell-K562)
25
20
15
10
5
0
Unaffected Sibling
Pt 2.2
Pt 2.1
*
*
*
*
Resting
10 min
30 min
60 min
Time (minutes)
F
% K562 specific lysis
30
25
20
15
10
5
0
0
10
20
30
40
50
NKL cell to Target cell Ratio
NKL Cells
WT #5
HEM1 KO#1
HEM1 KO#2
HEM1 KO#3
G
IFNγ
Gzm B
WT Clones
HEM1 KO clones
% of ctrl
200
150
100
50
0
*
**
No Stim
NKG2D/2B4

Figure S7. Patient T cells and neutrophils show migratory and morphological abnormalities and HEM1-deficient NK cells show reduced killing and conjugation. (**A**) Photomicrographs of $CD4^+$ T cell blasts from normal controls (NC) or patients (Pt) spontaneously migrating on ICAM-1 and imaged in real time using differential interference contrast (DIC) or fixed and stained with phalloidin (F-actin). Red arrows: abnormal formin-bundled actin spikes. Orange arrows: WASp-mediated actin puncta. Scale bar: 2 μm. (**B**) Spontaneous velocity of individual T cells migrating as in (A). **C**) Individual tracks of neutrophils migrating in response to the labeled chemoattractant (expansion of Fig. 2A), color-coded to show the cellular displacement at different time intervals. (**D**) Modified Boyden chamber migration assay comparing Pt 1.1 neutrophils to daily control and normal range (historic controls) for a range of chemoattractants. (**E**) Fraction of NK cells from Pts 2.1 and 2.2 sustained in conjugates at the indicated times compared to their unaffected heterozygous sibling and normalized to a healthy donor. (**F**) Lysis of K562 target cells by parental NKL cells, an NK92 control, a WT clone, and three HEM1 KO clones at the indicated effector-target ratios. (**G**) Secretion of IFNγ and granzyme B by NKL WT clones HEM1-deficient clones stimulated with agonistic antibodies against 2B4 and NKG2D for 18 hours. Data represent at least three independent experiments. Statistical analysis was performed using a Wilcoxon matched-pairs signed-rank test [$*P \leq 0.05$, $**P \leq 0.01$.]

Figure S8.

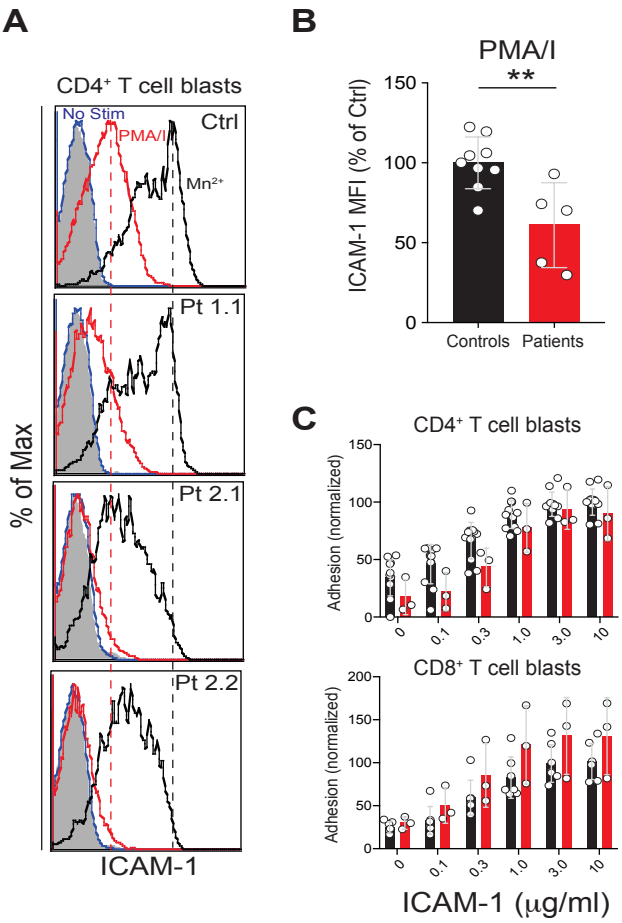
A
CD4⁺ T cell blasts
No Stim
PMA/I
Ctrl
Mn²⁺
Pt 1.1
Pt 2.1
Pt 2.2
% of Max
ICAM-1
B
PMA/I
**
ICAM-1 MFI (% of Ctrl)
150
100
50
0
Controls
Patients
C
CD4⁺ T cell blasts
Adhesion (normalized)
150
100
50
0
0
0.1
0.3
1.0
3.0
10
CD8⁺ T cell blasts
Adhesion (normalized)
200
150
100
50
0
0
0.1
0.3
1.0
3.0
10
ICAM-1 (μg/ml)

Figure S8. Patient T cells have defective integrin signaling and high concentration ICAM-1 improves adhesion. (**A**) Representative histograms of soluble fluorochrome-labelled ICAM-1 binding following no stimulation, 10 min of phorbol myristate acetate (PMA)/Ionomycin (I) stimulation, or manganese (Mn^{2+}) - induced integrin activation in CD4+ T cell blasts. (**B**) Averages of mean fluorescence intensity (MFI) of soluble labelled-ICAM-1 binding to PMA/I-stimulated cells normalized to the control average, as shown in (A). (**C**) $CD4^+$ and $CD8^+$ T cell blasts adhering to the indicated dose of immobilized ICAM-1. Values were normalized to the average of the maximum control response. (**D**) Combined results of three independent experiments showing CD69 and CD25 upregulation on purified Ctrl and Pt naïve CD4+ T cells over a range of anti-CD3 stimulation doses with 1 μg/ml anti-CD28 in the presence or absence of 1 μg/ml ICAM-1. (**E**) Proliferation index of control and patient naive $CD4^+$ T cell proliferation 5 days post-stimulation with the indicated dose of anti-CD3 and ICAM-1/anti-CD28 (1 μg/ml each). Statistical analyses for (B), (C), and (D) were performed using a *t*-test without assuming equal variance. All data represent at least 3 independent experiments. [*$P \leq 0.05$, **$P \leq 0.01$.]

Figure S9.

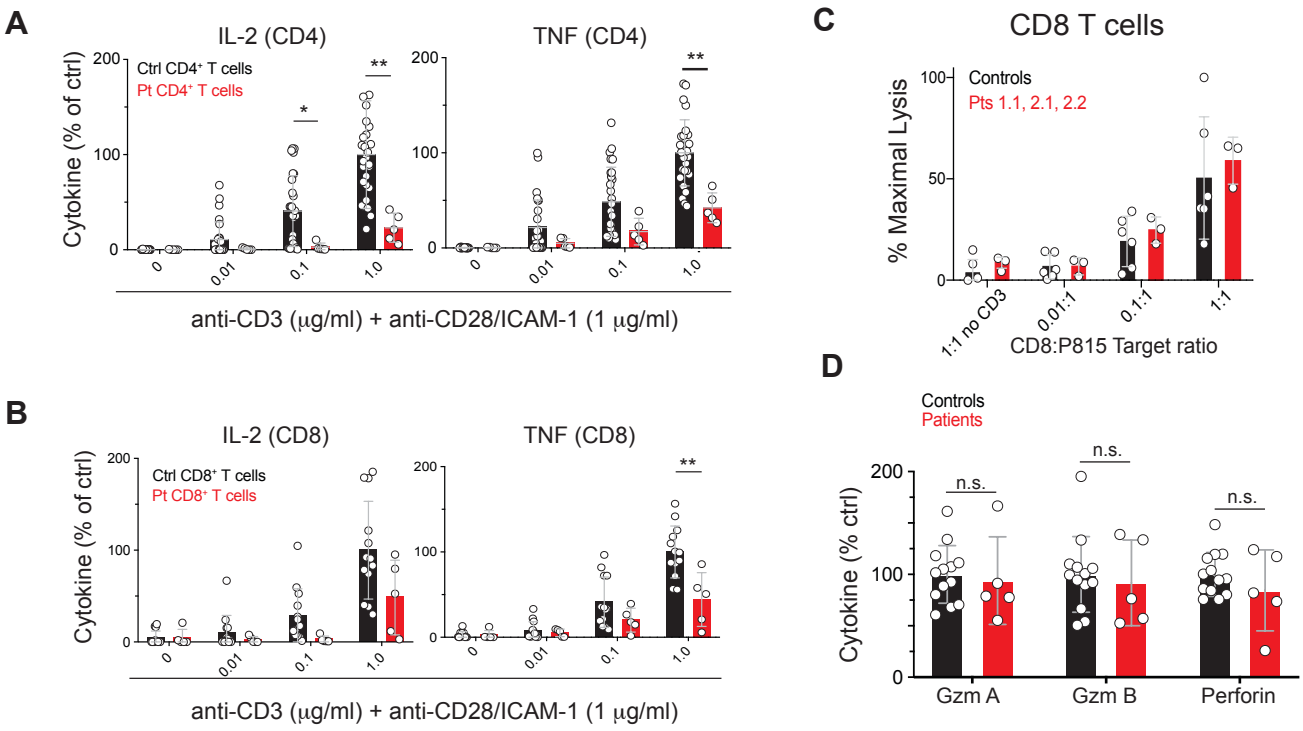
A
IL-2 (CD4)
TNF (CD4)
Ctrl CD4+ T cells
Pt CD4+ T cells
Cytokine (% of ctrl)
anti-CD3 (μg/ml) + anti-CD28/ICAM-1 (1 μg/ml)
B
IL-2 (CD8)
TNF (CD8)
Ctrl CD8+ T cells
Pt CD8+ T cells
C
CD8 T cells
Controls
Pts 1.1, 2.1, 2.2
% Maximal Lysis
1:1 no CD3
0.01:1
0.1:1
1:1
CD8:P815 Target ratio
D
Controls
Patients
n.s.
Gzm A
Gzm B
Perforin

Figure S9. Patient T cells show selective defects in T cell receptor induction of cytokine expression and proliferation. (**A**) IL-2 and TNF secretion by purified $CD4^+$ T cell blasts after stimulation for 36 hours with immobilized ICAM-1/anti-CD28 and the indicated dose of anti-CD3. (**B**) IL-2 and TNF secretion by $CD8^+$ T cell blasts upon restimulation for 36 hours with immobilized ICAM-1/anti-CD28 and the indicated dose of anti-CD3. (**C**) Lysis of P815 target cells coated with 1 μg/ml anti-CD3 and incubated at different ratios with $CD8^+$ T cell blasts derived from Pts or controls. (**D**) Granzyme (Gzm) and perforin secretion by $CD8^+$ T cell blasts after stimulation for 36 hours with immobilized ICAM-1/anti-CD28 and the indicated dose of anti-CD3. n.s.: not significant. Data represent at three independent experiments. All statistical analyses were performed using a *t*-test without assuming equal variance. [*$P \leq 0.05$, **$P \leq 0.01$.]

Figure S10.

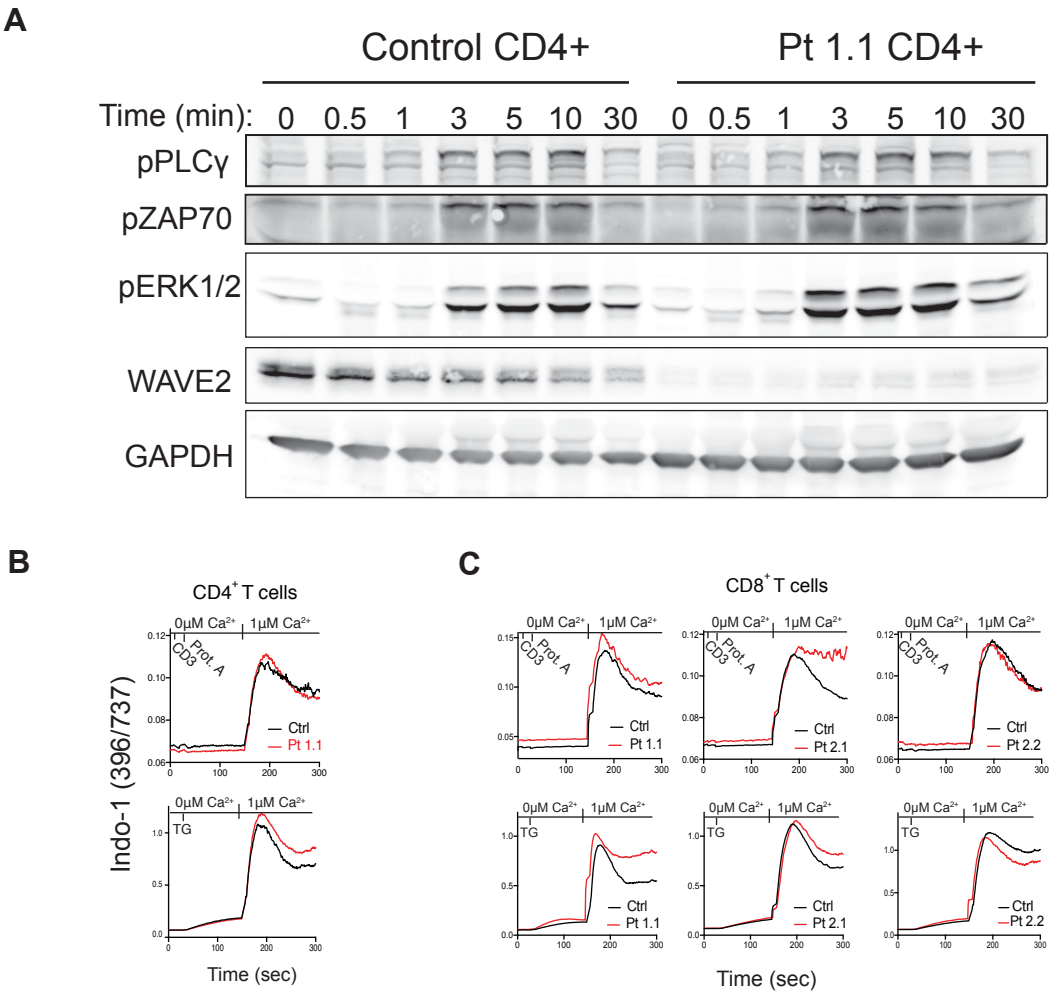
A
Control CD4+
Pt 1.1 CD4+
Time (min): 0 0.5 1 3 5 10 30 0 0.5 1 3 5 10 30
pPLCγ
pZAP70
pERK1/2
WAVE2
GAPDH
B
CD4+ T cells
0μM Ca2+
1μM Ca2+
CD3
Prot. A
TG
Ctrl
Pt 1.1
Indo-1 (396/737)
Time (sec)
C
CD8+ T cells
Pt 2.1
Pt 2.2
Time (sec)

Figure S10. Normal TCR-induced tyrosine phosphorylation on proximal targets and normal Ca^{2+} flux in patient T cells. (**A**) Immunoblots for the indicated T cell signaling proteins (p indicates the phosphorylated version) using lysates from purified normal control and patient $CD4^+$ T cell blasts rested and restimulated for the indicated time with soluble anti-CD3/CD28 (1 μg/ml each). (**B**) Calcium flux using the ratiometric dye INDO-1 in Pt and Ctrl $CD4^+$ T cell blasts following stimulation with anti-CD3 and Protein A crosslinking (top) or thapsigargin (TG)-induced depletion of ER-calcium stores (bottom). (**C**) Calcium flux in Pt and Ctrl $CD8^+$ T cell blasts following stimulation as in (B). Data represent at least 3 independent experiments.

Figure S11.

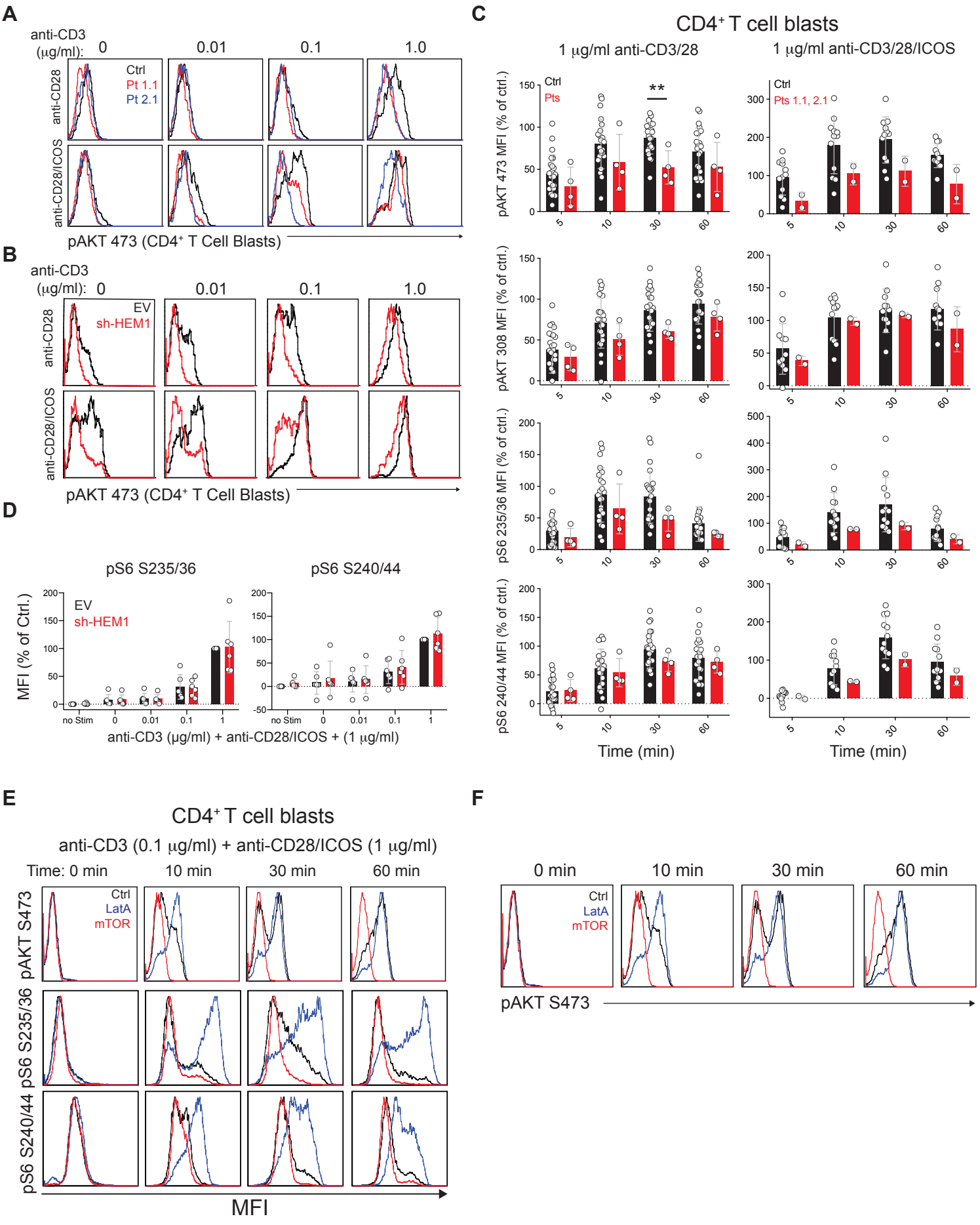
A
anti-CD3 (μg/ml): 0 0.01 0.1 1.0
anti-CD28
anti-CD28/ICOS
Ctrl
Pt 1.1
Pt 2.1
pAKT 473 (CD4+ T Cell Blasts)
B
anti-CD3 (μg/ml): 0 0.01 0.1 1.0
anti-CD28
anti-CD28/ICOS
EV
sh-HEM1
pAKT 473 (CD4+ T Cell Blasts)
C
CD4+ T cell blasts
1 μg/ml anti-CD3/28
1 μg/ml anti-CD3/28/ICOS
pAKT 473 MFI (% of ctrl.)
pAKT 308 MFI (% of ctrl.)
pS6 235/36 MFI (% of ctrl.)
pS6 240/44 MFI (% of ctrl.)
Ctrl
Pts
Pts 1.1, 2.1
**
Time (min)
D
pS6 S235/36
pS6 S240/44
MFI (% of Ctrl.)
EV
sh-HEM1
no Stim
anti-CD3 (μg/ml) + anti-CD28/ICOS + (1 μg/ml)
E
CD4+ T cell blasts
anti-CD3 (0.1 μg/ml) + anti-CD28/ICOS (1 μg/ml)
Time: 0 min 10 min 30 min 60 min
pAKT S473
pS6 S235/36
pS6 S240/44
Ctrl
LatA
mTOR
MFI
F
0 min 10 min 30 min 60 min
Ctrl
LatA
mTOR
pAKT S473

Figure S11. Patient T cells have selective defects in AKT phosphorylation indicating a defect in mTORC2 kinase activity. (**A**) Extended dose response showing pAKT473 induction in $CD4^+$ control and patient T cell blasts (A) or (**B**) empty vector (EV) and HEM1 sh-RNA (sh- HEM1) (B) transduced purified CD4 T cell blasts with anti-CD3/CD28 stimulation in the absence (top) or presence (bottom) of anti-ICOS (1 μg/ml) as in Fig. 4A. (**C**) Time course of AKT and S6 phosphorylation in purified $CD4^+$ control and patient T cell blasts stimulated with 1 μg/ml anti-CD3/CD28 with or without 1 μg/ml anti-ICOS, as measured by flow cytometry. Shown are the mean fluorescence intensity (MFI) values for each phospho-protein stain normalized to the maximal control response across four experiments. Statistical analysis was performed using a *t*-test without assuming equal variance. (**D**) Dose response quantifying MFI of S6 phosphorylated on Ser235/36 and Ser240/44 in purified T cell blasts transduced with empty vector (EV) or sh-HEM1 in six independent experiments. (**E**) and (**F**) Representative flow plots of phosphoproteins in purified $CD4^+$ T cell blasts treated with either 1 μM LatA or 10 μM Ku-0063794 (mTOR) inhibitors prior to stimulation with anti-CD3/CD28/ICOS for the indicated time. Data represent at least three independent experiments. [$^{**}P \leq 0.01$.]

Figure S12.

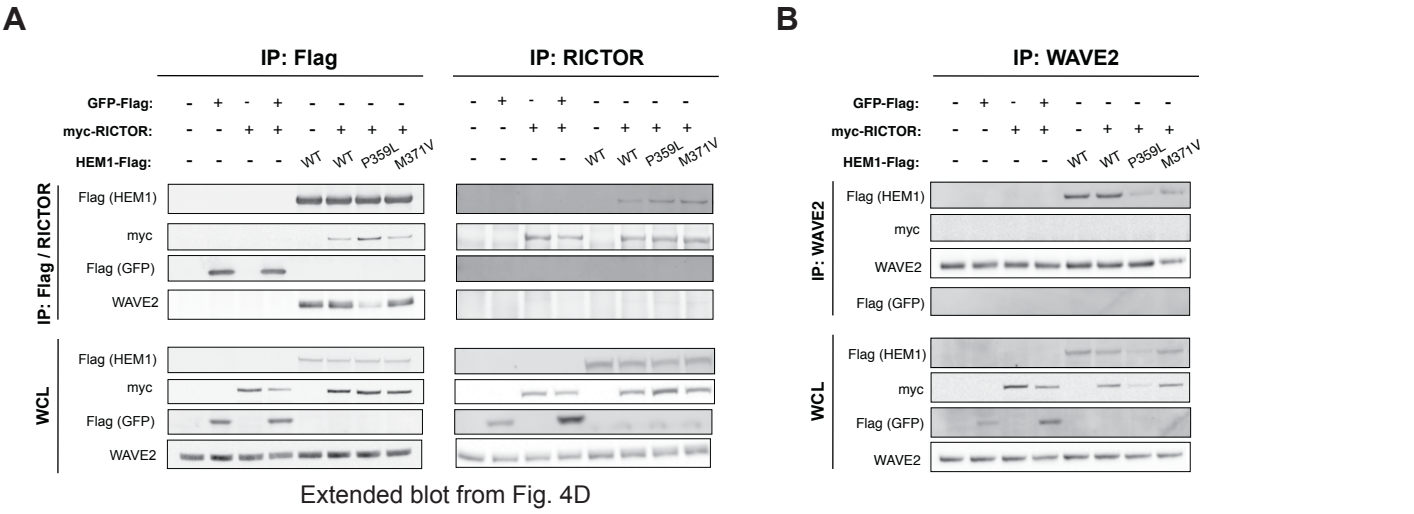

Extended blot from Fig. 4D

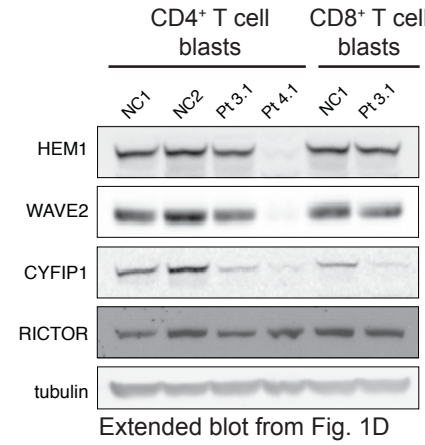

Extended blot from Fig. 1D

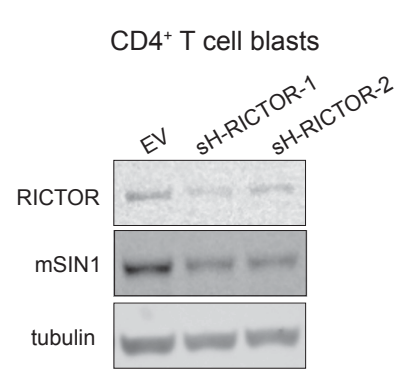

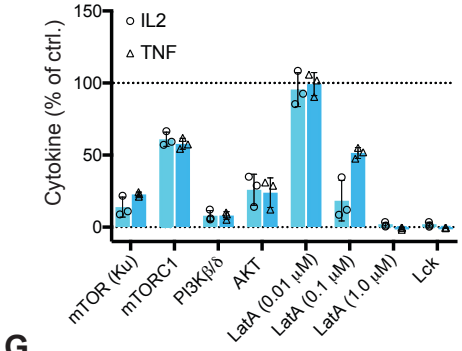

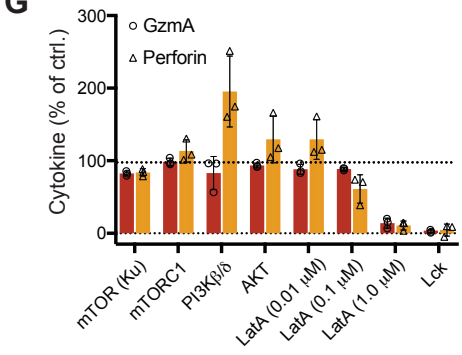

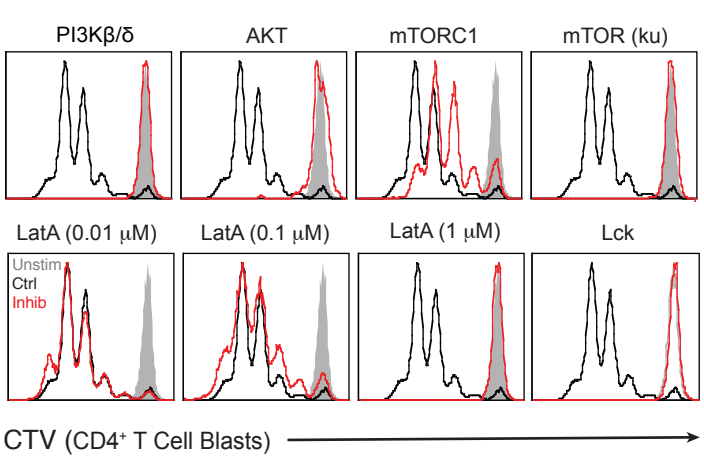

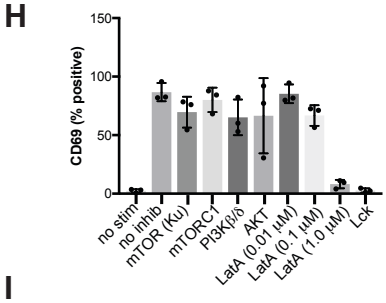

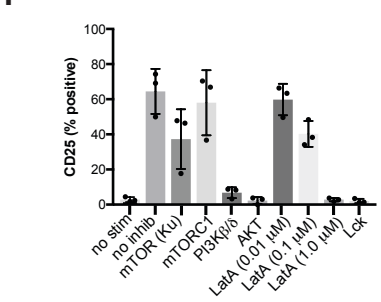

Figure S12. HEM1 interacts with RICTOR outside of the WRC and RICTOR KO recapitulates patient T cell defects. (A) Extended immunoblot of the FLAG and RICTOR IP from Figure 4D showing additional control lanes. (**B**) WAVE2 IP from 293T cells transduced with lentiviruses expressing myc-RICTOR and either FLAG-tagged GFP or FLAG-tagged HEM1 (WT or mutant) and blotted for the indicated targets. (**C**) WRC component and RICTOR expression in patient and normal control (NC) CD4+ and CD8+ T cell blasts. Extended from Fig. 1D. Importantly, HEM1-deficient patient cells expressed normal levels of RICTOR, indicating that HEM1 is not required for the stability of RICTOR or mTORC2. (**D**) Immunoblot showing efficiency of shRNA-mediated RICTOR knockdown in purified $CD4^+$ T cell blasts relative to empty vector (EV) control. Also shown is mSIN1, a component of mTORC2, that is destabilized by the loss of RICTOR. (**E**) and (**G**) Cytokine production in normal $CD8^+$ T cell blasts following an 18-hour stimulation with anti-CD3/28/ICAM1 (1 μg/ml each) coated surfaces and co-treatment with chemical inhibitors of the indicated signaling molecules or the indicated doses of latrunculin A (LatA). mTOR = 10 μM KU0063794, mTORC1 = 1 μM rapamycin, PI3K = 100 μM AZD8186, AKT = 10 μM MK2206, Lck = 10 μM LckI. As controls, inhibition of TCR signaling by blocking Lck kinase or complete disruption of filamentous actin with high dose LatA arrested proliferation and release of granule contents. (**F**) Cell Trace Violet (CTV) plots showing proliferation of purified $CD4^+$ T cell blasts after stimulation and treatment as in (E). (**H**) and (**I**) CD69 and CD25 expression on naïve $CD4^+$ T cells from a normal donor stimulated with platebound anti-CD3/28/ICAM1 (1 μg/ml each) in the presence of the indicated inhibitors for 36 hours. Data represent at least three independent experiments.

Captions for Supplemental Items

Table S3. Evaluation of key immunological subsets (separate file)

Table S5. IP/Mass-spec analysis of Hem1 and Wave2 interacting proteins (separate file)
(Tab1) Proteins identified from Wave2 IP or Flag IP from either JKE6.1 cells knocked out for Wave2 or Wave2, Hem1-KO JKE6.1 cells reconstituted with WT Hem1-Flag or M371V Hem1-Flag, digested, and then labeled with Low, Med, and High isotope tags, respectively. **(Tab2)** Proteins identified from Isotype or Wave2 IP from primary $CD4^+$ T cell blasts derived from PBMCs of a healthy donor. **(Tab3)** Proteins identified from Wave2 IP from either JKE6.1 cells knocked out for Wave2, Hem1-KO JKE6.1 cells reconstituted with WT Hem1-Flag or M371V Hem1-Flag, digested, and then labeled with Low, Med, and High tags, respectively. Proteins above a Ratio of 1.5 and Log_2 difference of 1.0 are shown. **(Tab4)** Proteins identified from Flag IP from either JKE6.1 cells knocked out for Hem1, Hem1-KO JKE6.1ells reconstituted with WT Hem1-Flag or M371V Hem1-Flag, digested, and then labeled with Low, Med, and High epitope tags, respectively. Proteins above a Ratio of 1.5 and Log_2 difference of 1.0 are shown. **(Tab5)** Proteins identified from Isotype or Wave2 IP from primary $CD4^+$ T cell blasts derived from PBMCs of a healthy donor. Proteins above a ratio of 1.5 and a probability score of 1.0 are shown. **(Tab6)** A list of proteins positively identified as interacting with both Hem1 and Wave2 in Jurkat Cells and Wave2 in primary cells.

Movie S1.
Primary $CD4^+$ T cell blasts from a normal control or Pt 1.1 transfected with Lifeact-GFP and spreading on stimulatory coverslips coated with 1 μg/ml antiCD3/28 and 1 μg/ml ICAM-1.

Movie S2.
Hem-1 deficient clone derived from JKE6.1 parental cells, and transduced with Lifeact-GFP expressing virus as well as either WT Hem1-Flag, P359VLHem1-Flag, M371V Hem1-Flag, or V519L Hem1-Flag. Cells are spreading on stimulatory coverglass coated with 1 μg/ml antiCD3 and 1 μg/ml ICAM-1.

Movie S3.
Normal control or patient $CD4^+$ T cells migrating spontaneously on coverslips coated with 1 μg/ml ICAM-1.

Movie S4.
Normal control neutrophils (top) or patient 1.1 neutrophils (bottom) migrating in an EZ-TAXIScan chemotaxis chamber in response to either no chemoattractant (left), fMLF (center), or C5a (right).

Table S1. Actin-related primary immunodeficiencies

	WASp/WIP	ArpC1B	DOCK2	DOCK8	Rac2	Rac2	Moesin	RasGRP1	Coronin 1A	Hem1
Actin-related function	downstream of CDC42, activator of Arp2/3	component of Arp2/3 complex	Rac1 GEF	CDC42 GEF	GTPase, actin/NADPH oxidase function	GTPase, actin/NADPH oxidase function	links actin to transmembrane proteins	Ras GEF with DAG-binding domain	promote actin polymerization	WRC activation of Arp2/3, mTOR signaling
Genetic abnormality				Homozygous LOF	Heterozygous dominant negative	Homozygous LOF	X-linked LOF	Homozygous LOF	Compound heterozygous LOF	Homozygous/Heterozygous LOF
Immunodeficiency										
Defective T cell activation	yes	yes (proliferation)	yes	yes, CD8	Yes (differentitation)	N/R	yes	yes	Yes (survival)	yes
Defective T cell Migration	yes	yes	yes	yes (3D only)	N/R	N/R	yes	Yes	yes	yes
Recurrent infections	yes	yes	yes	yes	yes	Yes	yes	yes	yes	yes
Bronchiectasis	Yes	mild	N/R	Yes	N/R	Yes	N/R	yes	yes	yes
Decreased NK cells	N/R	N/R	N/R	Yes	N/R	No	yes	N/R	yes	yes
Decreased NK cytotoxicity	yes	yes	yes	yes	N/R	N/R	N/R	yes	N/R	yes
Neutrophil Migration Defects	yes	yes	yes	yes	yes	N/R	N/R	N/R	N/R	yes
Antibody Abnormalities	Elevated IgA, low IgM	Elevated IgA/IgE, auto-antibodies	low specific antibody production, hyper IgM	variable IgM	Low to normal	hypogammaglobulinemia	hypogammaglobulinemia	hyper IgA, poor specific antibody responses	variable hypogammaglobulinemia	hyper IgG, poor specific responses
Atopy/allergic hyperreactivity										
Atopic Disease	food allergies	food allergies	yes	food allergy, eczema	N/R	allergic urticaria/food allergy	N/R	N/R	N/R	yes
Elevated IgE	yes	yes	Yes (1 patient)	Yes	N/R	No	N/R	N/R	Yes	yes
Excess adaptive immune responses										
Increased B cell number	N/R	yes	No (B cell lymphopenia)	N/R	N/R	No, decreased	N/R	yes (transitional and CD21low)	N/R	yes
Increased memory T cells or activated T cells	N/R	N/R	Yes (lymphopenia-induced expansion)	N/R	Yes (senescent)	No	N/R	yes	N/R	yes
Hepatomegaly	Mild/Rare	yes	Yes	Yes (some patients)	N/R	N/R	N/R	Yes	N/R	yes
Splenomegaly	N/R	yes	N/R	N/R	N/R	N/R	N/R	yes	N/R	yes
Lymphadenopathy	N/R	N/R	N/R	N/R	N/R	Yes	N/R	Yes	N/R	yes
Autoimmune disease	frequent	yes	N/R	yes	N/R	No	N/R	Yes	N/R	yes
Syndromic Features										
Other Features	thrombocytopenia, eczema, nephropathy, congenital neutropenia	microthrombocytopenia, eosinophilia, inflammatory disease, bleeding tendency and vasculitis, eczema		Early-onset invasive bacterial and viral infections. Decreased TRECS at birth, stretched cell phenotype, and ear infections	recurrent abcesses, neutrophilia, leukocytosis	membranous glomerulonephritis and kidney failure	recurrent molluscum, eczema, lymphopenia, fluctuating monocytopenia and neutropenia, and susceptibility to VZV.	B cell proliferation and activation defect. Improves with lenalidomide treatment	EBV-associated lymphoproliferation, mucocutaneous immunodeficiency	destructive ear infections, EBV-driven lymphoproliferative disease
References:	https://www.sciencedirect.com/science/article/pii/S0091674906003162?via%3Dihub.	https://www.nature.com/articles/ncomms14816, https://www.jacionline.org/article/S0091-6749(16)31453-1/pdf, http://www.bloodjournal.org/content/132/22/2362.long?sso-checked=true, https://www.jacionline.org/article/S0091-6749(19)30206-4/fulltext https://www.jacionline.org/article/S0091-6749(19)30206-4/pdf	https://www.nejm.org/doi/10.1056/NEJMoa1413462, https://www.nature.com/articles/5090591	https://www.nejm.org/doi/10.1056/NEJMoa0905506?url_ver=Z39.88-2003&rfr_id=ori:rid:crossref.org&rfr_dat=cr_pub%3dwww.ncbi.nlm.nih.gov, https://www.jacionline.org/article/S0091-6749(13)00004-3/abstract	https://www.ncbi.nlm.nih.gov/pmc/articles/PMC1828/	https://www.jacionline.org/article/S0091-6749(14)01581-4/pdf	https://www.sciencedirect.com/science/article/pii/S0091674916340427?via%3Dihub	https://www.nature.com/articles/ni.3575	https://www.ncbi.nlm.nih.gov/pubmed/18836449, https://www.ncbi.nlm.nih.gov/pubmed/25073507; doi: 10.1038/ni.1662; 10.1016/j.jaci.2013.01.042.	This paper

N/R = not reported in literature to be associated with the indicated inborn error of immunity

EBV = Epstein-Barr virus

LOF = loss of function

TREC = T cell receptor excision circle

Table S2. Clinical characteristics of patients with HEM1 mutations

Patient demographics	**Pt. 1.1**	**Pt. 2.1**	**Pt. 2.2**	**Pt. 3.1**	**Pt. 4.1**
Current age (6/2019) (yrs)	11	17	10.5	11.5	2.5
Onset of symptoms	9 months	6 months	11 Months	13 Months	12 months
Immunodeficiency					
Defective T cell activation	Yes	Yes	Yes	Yes	Yes
Skin infections	Yes, recurrent (bacterial)	Yes, one episode (bacterial)	Yes, one episode (bacterial)	Yes, recurrent (viral)	No
Recurrent ear infections	Yes	Yes, destructive	Yes, destructive	Yes, destructive with mucoid effusion	Yes
Recurrent pneumonia	Yes (necrotizing)	Yes	Yes	No	Yes
Bronchiectasis	Yes	Yes	Yes	No	Yes
Decreased NK cells	Yes	Yes	Yes	N/D	N/D
Decreased NK cytotoxicity	Yes	Yes	Yes	N/D	N/D
Neutrophil Migration Defects	Yes	N/D	N/D	Yes	N/D
Antibody Abnormalities	Hyper IgG	Hyper IgG, Low IgM/IgA	Hyper IgG, auto antibodies	Low Specific antibody production	Poor EBV-specific antibody production
Other infections	Septic arthitis, bacteremia	Cellulitis	Bacteremia, Rosai-Dorfman disease associated with recurrent infection	Bacteremia, invassive and disseminated HSV1, molluscum contagiosum, pseudomonas aeruginosa with recurrent high fever, roseola infantum	Recurrent EBV-driven HLH, severe pyelonephritis, severe gastroenteritis
Failure to thrive	No	Yes	No	No	Yes
Atopy/allergic hyperreactivity					
Asthma symptoms	Yes	Yes	Yes	Yes, food allergies	Yes
Hyper IgE	Yes	No	Yes	N.D.	Yes
Excess adaptive immune responses					
Increased B cell number	Yes	Yes	Yes	No	No
Increased memory T cells or activated T cells	Yes	Yes	Yes	N/D	Yes
Hepatomegaly	Yes	Yes	Yes	Yes	Yes
Splenomegaly	Yes	Yes	Yes	Yes	Yes
Lymphadenopathy	Yes, recurrent	Yes	Yes, recurrent	No	No
Autoimmune disease	No	No	Immune complex glomerulonephritis, SLE/Lupus-like disease	ITP post- MMR vaccination	HLH-like disease
Syndromic Features					
Dention Problems	Yes, poor dentition	No	No	Yes, primary teeth retention	No
Other Features	Pectus carinatum, trivial tricuspid valve deficiency	No	No	Obesity, bleeding tendencies with gum and skin bruising, Similar features observed in *NCKAP1L* variant negative siblings	Intracerebral ventricular dilatation (unilateral) + ventricular heterotopia, liver calcification (liver hamartoma), kidney dilatation, cardiomegaly and muscular ventricular septal defect with dilatation of the ascending aorta, aortic bicuspidia, liver cysts, oral feeding issues and gastric tube.

Table S4. Homozygous non-synonymous variants observed in patients.

Patient	Gene	Allele Status	Variant	DNA Change	Protein Change	Impact
Pt 1.1	*NCKAP1L*	Homozygous Alt.	chr12:54910757C>T	c.1076C>T	p.Pro359Leu	missense
Pt 1.1	*HOXC8*	Homozygous Alt.	chr12:54403334A>G	c.266A>G	p.Tyr89Cys	missense
Pt 1.1	*ANO10*	Homozygous Alt.	chr3:43647217T>C	c.128A>G	p.Lys43Arg	missense
Pt 1.1	*MITD1*	Homozygous Alt.	chr2:99787009C>T	c.584G>A	p.Arg195Gln	missense
Pt 1.1	*PPP2R3A*	Compound Het.	chr3:135745741C>A	c.2063C>A	p.Pro688His	missense
Pt 1.1	*PPP2R3A*	Compound Het.	chr3:135789386A>G	c.2536A>G	p.Ile846Val	missense
Pt 3.1	*TENM2*	Homozygous Alt.	chr5:167689441G>A	c.7924G>A	p.Val2642Met	missense
Pt 3.1	*GPR84*	Homozygous Alt.	chr12:54756641T>C	c.995A>G	p.Tyr332Cys	missense
Pt 3.1	*OR51D1*	Homozygous Alt.	chr11:4661442A>C	c.422A>C	p.His141Pro	missense
Pt 3.1	*RUBCNL*	Homozygous Alt.	chr13:46924321T>C	c.1025A>G	p.His342Arg	missense
Pt 3.1	*NCKAP1L*	Homozygous Alt.	chr12:54911332A>G	c.1111A>G	p.Met371Val	missense
Pt 3.1	*WNT1*	Homozygous Alt.	chr12:49373410T>A	c.264T>A	p.Ser88Arg	missense
Pt 3.1	*HMMR*	Homozygous Alt.	chr5:162896779A>G	c.406A>G	p.Thr136Ala	missense
Pt 3.1	*TRIM34*	Homozygous Alt.	chr11:5664062G>A	c.890G>A	p.Arg297Gln	missense
Pt 3.1	*PCDHGA5*	Homozygous Alt.	chr5:140744676G>T	c.779G>T	p.Arg260Leu	missense
Pt 4.1	*FRAS1*	Homozygous Alt.	chr4:79240131A>T	c.2128A>T	p.ILe710Leu	missense
Pt 4.1	*NCKAP1L*	Homozygous Alt.	chr12:54905624G>T	c.773G>T	p.Arg259Leu	missense
Pt 4.1	*KIR3DL1*	Homozygous Alt.	chr19:55331298AG>A	c.486delG	p.Lys162X	frameshift
Pt 4.1	*KIR3DL1*	Homozygous Alt.	chr19:55331299G>A	c.487G>A	p.Asp163Asn	missense

Table S6. Antibodies used in this study

Target	Purpose	Dilution	Conjugate	Source	Cat #	Clone
WAVE2	Immunoblot/IP/Flow	1:2000 / 2.5 ug per mg input / 1:50	None	Cell Signaling Technology	3659	D2C8
NCKAP1L	Immunoblot	1:1000	None	Thermo FIsher	PA5-58813	
Flag	Immunoblot/IP	1:50 / 5 ug per mg input	None	Sigma	F1804	M2
GAPDH	Immunoblot	1:2000	None	Cell Signaling Technology	2118	14C10
mTOR	Immunoblot	1:1000	None	Cell Signaling Technology	2972S	
Rictor	Immunoblot	1:1000	None	Cell Signaling Technology	2114S	53A2
Rictor	IP	2.5 ug per mg input	None	Bethyl	A300-458A	
Deptor	Immunoblot	1:1000	None	Cell Signaling Technology	11816	D9F5
Raptor	Immunoblot	1:1000	None	Cell Signaling Technology	2280S	24C12
CYFIP1	Immunoblot	1:1000	None	EMD Millipore	07-531	
p-PLCy (Y783)	Immunoblot	1:1000	None	Cell Signaling	2821S	
p-ERK1/2 (Y202/204)	Immunoblot	1:2000	None	Cell Signaling Technology	4370	D.13.14.4E
AKT	Immunoblot	1:500	None	Cell Signaling Technology	2920	40D4
p-AKT S473	Immunoblot	1:1000	None	Cell Signaling Technology	4058	193H12
p-GSK3a/b (S21/9)	Immunoblot	1:1000	None	Cell Signaling Technology	8566	D17D2
GSK3a	Immunoblot	1:1000	None	Cell Signaling Technology	4337	D80E6
Anti-Rabbit IgG	Immunoblot	1:15000	HRP	Southern Biotech	4050-05	
Anti-Mouse IgG	Immunoblot	1:15000	HRP	Southern Biotech	1030-05	
Anti-Mouse IgG	Immunoblot	1:15000	AlexaFluor Plus 680	Thermo Fisher	A32729	
Anti-Rabbit IgG	Immunoblot	1:15000	AlexaFluor Plus 800	Thermo Fisher	A32735	
CD3	Stimulation	0.01 - 1.0 ug/ml	None	Biolegend	300332	Hit3a
CD28	Stimulation	1.0 ug/ml	None	Biolgend	302934	CD28.2
CD278/ICOS	Stimulation	1.0 ug/ml	None	Biolgend	313511	C398.4A
pAKT (308)	Flow Cytometry	1:100	Alexa Fluor 488	Cell Signaling Technology	43506S	D25E6
pAKT (473)	Flow Cytometry	1:100	Alexa Fluor 647	Cell Signaling Technology	4075S	D9E
pS6 (235/36)	Flow Cytometry	1:100	PE	Cell Signaling Technology	5316S	D57.2.2E
pS6 (240/44)	Flow Cytometry	1:100	Alexa Fluor 647	Cell Signaling Technology	5044S	D68F8
pSTAT3	Flow Cytometry	1:100	PE	Biolegend	651004	13A3-1
pSTAT5	Flow Cytometry	1:100	Alexa Fluor 647	BD Biosciences	612599	47/Stat5
CD107a	Flow Cytometry	1:100	Alexa Fluor 488	Biolegend	328610	H4A3
Granzyme A	Flow Cytometry	1:100	APC	Biolegend	507220	CB9
Granzyme B	Flow Cytometry	1:100	PE	Biolegend	372208	QA16A02
TNF	Flow Cytometry	1:100	Alexa Fluor 647	Biolegend	502916	MAb11
Perforin	Flow Cytometry/Microscopy	1:100	Alexa Fluor 488	Biolegend	308108	dG9
IFNy	Flow Cytometry	1:100	Alexa Fluor 488	Biolegend	502515	4S.B3
IL2	Flow Cytometry	1:100	Alexa Fluor 647	Biolegend	500315	MQ1-17H12
Anti-Human IgG	ICAM-1 immobilization	2 ug/ml	None	Jackson ImmunoResearch	109-005-008	
F(ab')2 anti-human IgG	ICAM-1 crosslinking	1 ug/m	Alexa Fluor 647	Jackson ImmunoResearch	109-606-098	
CD3	NK conjugate assay	40 ug/ml, 1 ul per test	BV711	Biolegend	317328	OKT3
CD56	NK conjugate assay	100 ug/ml, 2 ul per test	BV605	Biolegend	318334	HCD56
Goat anti-rabbit IgG	NK synapse analysis	1:1000	Alexa Fluor 568	Thermo Fisher	A11011	